

**LEAD ISOTOPE GEOCHEMISTRY OF Pb-Zn DEPOSITS  
FROM EASTERN TAURIDES, TURKEY**

**A THESIS SUBMITTED TO  
THE GRADUATE SCHOOL OF NATURAL AND APPLIED SCIENCES  
OF  
THE MIDDLE EAST TECHNICAL UNIVERSITY**

**BY**

**NURİ CEYHAN**

**IN PARTIAL FULLFILMENT OF THE REQUIREMENTS FOR THE DEGREE OF  
MASTER OF SCIENCE  
IN  
THE DEPARTMENT OF GEOLOGICAL ENGINEERING  
DECEMBER 2003**

Approval of the Graduate School of the Natural and Applied Sciences

---

Prof. Dr. Canan Özgen  
Director

I certify that this thesis satisfies all the requirements as a thesis for the degree of  
Master of Sciences.

---

Prof. Dr. Asuman Türkmenoğlu  
Head of the Department

This is to certify that we have read this thesis and that in our opinion it is fully  
adequate, in scope and quality, as a thesis for the degree of Master Sciences.

---

Prof. Dr. Nilgün Güleç  
Supervisor

Examining Committee Members

Prof. Dr. Erdin Bozkurt

Assoc. Prof. Dr. Yusuf Kağan Kadioğlu

Asst. Prof. Dr. Pırl Önen

Bayram Artun

Prof. Dr. Nilgün Güleç

## **ABSTRACT**

### **LEAD ISOTOPE GEOCHEMISTRY OF Pb-Zn DEPOSITS**

#### **FROM EASTERN TAURIDES, TURKEY**

CEYHAN, Nuri

MSc, Department of Geological Engineering

Supervisor: Prof. Dr. Nilgün GÜLEÇ

December 2003

This study is concerned with the Pb-isotope compositions of galena samples from Pb-Zn occurrences in southern Turkey. The purpose is to i) provide chronologic information for ore deposition, ii) investigate the likely source(s) of lead in ore deposits, and iii) examine the possible control of tectonic setting and crustal basement on Pb-isotope compositions. The data used in the study belongs to the deposits located in Taurides (Zamantı, Kahramanmaraş, Malatya, Elazığ, Bitlis), with additional data from Niğde Massif and Hakkari Area.

The mineralizations are dominantly carbonate-hosted Pb-Zn deposits formed as fracture and karst fillings and, in some places, parallel to bedding. Ore minerals are mainly Zn-oxides and minor Zn, Pb-sulphides.

The Pb-isotope compositions, as evaluated in terms of their configuration with respect to reference crustal growth curves and reference isochrons on conventional Pb-isotope diagrams, point to U/Pb ratios greater than average crustal values (and close to the Western Mediterranean Crustal Growth Curve) for all the deposits, indicating upper crustal source for Pb. However, some of the deposits (Afşin-Kahramanmaraş; Oreks, Dünderlı, Ağcaşar and skarn type deposits to the south of Çadırkaya in Zamantı (Kayseri-Adana); Keban-Elazığ) appear to have magmatic inputs in their genesis. Relatively old deposits

are likely Paleozoic (Cafana-Malatya and Türksevin-Kahramanmaraş), Late Paleozoic-Early Mesozoic (Kaleköy-Zamantı) and Mesozoic (Hakkari) in age. The rest of the deposits (most of the occurrences in Zamantı, Niğde, Kahramanmaraş, Elazığ and Bitlis) are likely of Cenozoic age. The Pb-isotope compositions are, in general, similar to those from other occurrences in the Mediterranean Belt.

**Keywords:** Eastern Taurides, Pb isotope, Pb-Zn deposits, age of mineralization, source of mineralization

## ÖZ

### DOĞU TOROSLARDAKİ Pb-Zn YATAKLARININ

### KURŞUN İZOTOPU JEOKİMYASI, TÜRKİYE

**CEYHAN, Nuri**

Yüksek Lisans, Jeoloji Mühendisliği Bölümü

Tez Yöneticisi: Prof. Dr. Nilgün Güleç

Aralık, 2003

Bu çalışma Türkiye'nin güneyinde bulunan Pb-Zn zuhurlarından alınan galen örneklerinin Pb-izotop bileşimlerini konu almaktadır. Çalışmanın amacı i) cevherleşme yaşlarıyla ilgili bilgi sağlamak, ii) cevher yataklarındaki kurşunun olası kaynaklarını araştırmak, ve iii) tektonik konum ve kabuksal temelin cevherleşmedeki olası kontrolünü incelemektir. Bu çalışmada kullanılan veriler Toroslar'daki cevherleşmelere (Zamantı, Kahramanmaraş, Malatya, Elazığ, Bitlis) ek olarak, Niğde Masifi ve Hakkari bölgesinden elde edilmiştir.

Cevherleşmeler, genellikle karbonatlı kayalarda çatlak ve karst dolgusu ile yer yer de tabakaya uyumlu olarak gelişmiş Pb-Zn oluşumlarıdır. Cevher mineralleri egemen olarak Zn-oksit ve daha az olarak Zn, Pb-sülfid mineralleridir.

Pb-izotop bileşimleri, Pb-izotop diyagramlarında, referans kabuksal gelişim eğrileri ve referans izokronlar temel alınarak incelenmiştir. U/Pb oranı ortalama kabuk değerlerinden yüksek (ve Batı Akdeniz Kabuk Gelişim Eğrisine yakın) değerler olup Pb için üst kabuk kaynağını işaret etmektedir. Ancak bazı yataklar (Afşin-Kahramanmaraş; Zamantı bölgesindeki Oreks, Dünderlı, Ağcaşar ile Çadirkaya güneyindeki skarn tipi yataklar; Keban-Elazığ) magmatik katkı içermektedir. Yaşlı olan yataklar olasılıkla Paleozoyik (Cafana-Malatya and Türksevin-Kahramanmaraş), Geç Paleozoyik-Erken Mesozoyik (Kaleköy-Zamantı) ve Mesozoyik (Hakkari) yaşındadırlar. Diğer yataklar ise (Zamantı yataklarının çoğunluğu, Niğde, Kahramanmaraş, Elazığ ve Bitlis)

olasılıkla Senozoyik yaşlıdırlar. Genel anlamda, Pb-izotop bileşimleri Akdeniz kuşağındaki diğer cevherleşmelerle benzerlik göstermektedir

Anahtar Kelimeler: Doğu Toroslar, Pb-izotopları, Pb-Zn yatakları, cevherleşme yaşı, cevherleşme kaynağı

## ACKNOWLEDGEMENTS

I would like to express my sincere gratitude to my supervisor, Prof. Dr. Nilgün Güleç, for her support, suggestions and patience.

The major part of the research for this thesis was carried out with support by Teck Cominco Madencilik San. A. Ş., which I acknowledge with thanks.

I extend my thanks to Mr. Tayfun Cerrah, Mr. Bayram Artun and Mr. Uğur Kızıltepe for their support during various stages of this research.

Last but not the least, I thank to my parents for their encouragement and support.

## TABLE OF CONTENTS

<b>ABSTRACT.....</b>	<b>iii</b>
<b>ÖZ.....</b>	<b>v</b>
<b>ACKNOWLEDGEMENTS.....</b>	<b>vii</b>
<b>TABLE OF CONTENTS.....</b>	<b>viii</b>
<b>LIST OF TABLES.....</b>	<b>xi</b>
<b>LIST OF FIGURES.....</b>	<b>xii</b>
<b>CHAPTER</b>	
<b>1. INTRODUCTION.....</b>	<b>1</b>
1.1. Purpose and Scope.....	1
1.2. Methods of Study.....	2
1.3. Geographic Setting.....	2
1.4. Layout of Thesis.....	3
<b>2. TECTONIC SETTING AND REGIONAL GEOLOGY.....</b>	<b>5</b>
<b>3. OUTLINE OF GEOLOGY AND MINERALIZATION IN THE STUDIED AREAS.....</b>	<b>11</b>
3.1. Introduction.....	11
3.2. Studied Areas in Taurides.....	16
3.2.1. Zamantı Area.....	16
3.2.1.1. Geologic Outline.....	16
3.2.1.2. Mineralization.....	23
3.2.2. K. Maraş Area.....	26
3.2.2.1. Geologic Outline.....	26

3.2.2.2. Mineralization.....	26
3.2.3. Malatya Area .....	27
3.2.3.1. Geologic Outline.....	27
3.2.3.2. Mineralization.....	27
3.2.4. Keban Area.....	28
3.2.4.1. Geologic Outline.....	28
3.2.4.2. Mineralization.....	28
3.2.5. Bitlis Area.....	30
3.2.5.1. Geologic Outline.....	30
3.2.5.2. Mineralization.....	31
3.3. Studied Areas in Central Anatolian Crystalline Complex (CACC).....	33
3.3.1. Niğde Area.....	33
3.3.1.1. Geologic Outline.....	33
3.3.1.2. Mineralization.....	35
3.4. Studied Areas in the Arabian Platform.....	35
3.4.1. Hakkari Area.....	35
3.4.1.1. Geologic Outline.....	35
3.4.1.2. Mineralization.....	38
<b>4. BASIC PRINCIPLES OF Pb ISOTOPES.....</b>	<b>39</b>
4.1. Introduction.....	39
4.2. Basic Principles.....	39
4.3. Pb Isotope Geochemistry.....	42
4.4. Pb Isotopes in Ore Deposits.....	49
4.5. Homogeneous versus Heterogeneous Pb Sources.....	51

## **5. Pb-ISOTOPE COMPOSITIONS OF THE STUDIED**

<b>MINERALIZATIONS.....</b>	<b>54</b>
5.1. Introduction.....	54
5.2. Methods of Study.....	54
5.3. Results.....	55
<b>6. DISCUSSION.....</b>	<b>63</b>
6.1. Introduction.....	63
6.2. Pb-Isotope Compositional Groups: Implication as to the Age and Source of Mineralization.....	65
6.2.1. Group 1.....	68
6.2.2. Group 2.....	68
6.2.3. Group 3.....	69
6.2.4. Group 4.....	69
6.2.5. Group 5.....	70
6.2.6. Anomalous Compositional Group.....	71
6.3. Comparison with Pb-Isotope Data from Selected Countries.....	71
6.4. Final Comments.....	72
<b>7. CONCLUSIONS AND RECOMMENDATIONS.....</b>	<b>75</b>
<b>REFERENCES.....</b>	<b>77</b>

## **APPENDICES**

A. THE LOCATION AND GENERALIZED GEOLOGICAL MAP OF THE STUDIED AREAS (modified from 1/500 000 MTA maps, 1961).....	in pocket
--	-----------

## LIST OF TABLES

### TABLE

3.1	The information relevant to the outline of, and the mineralization in the studied areas with UTM coordinates of samples (Lmst: limestone, CRD: Carbonate replacement deposits, MVT: Mississippi Valley Type).....	12
4.1	Constants and symbols critical to Pb isotope geochemistry (Tosdal et al., 1999).....	44
4.2	Present-day U-Th-Pb compositions of the Crust-Mantle system (adapted from Allegre et al., 1988; Gariépy and Dupre, 1991).....	46
5.1.	Pb-Isotope results with relevant informations with UTM coordinates of samples (Lmst: limestone, CRD: Carbonate replacement deposits, MVT: Mississippi Valley Type) .....	56
6.1	Two-stage parameters for average active terrestrial lead (Stacey and Kramers, 1975).....	64
6.2	Two-stage parameters used by Ludwig (1989).....	64
6.3	Two-stage parameters used by Tosdal (2001).....	65

## LIST OF FIGURES

### FIGURE

- 1.1. Location map of the studied areas (1. Niğde area, 2. Zamantı area, 3. K. Maraş area, 4. Malatya area, 5. Elazığ area, 6. Bitlis area, 7. Hakkari area).....4
- 2.1. Simplified tectonic map showing major tectonic structures and tectonic provinces (Okay and Tüysüz, 1999). 1 is located in Kırşehir Massif, 2-6 are located in Taurides, 7 is located in Arabian Platform.....6
- 2.2. The geologic map showing the distribution of units in Taurides (Özgül, 1976).....8
- 2.3. Geologic map of Central Anatolian Crystalline Complex (Kadioğlu, et al., 2003).....9
- 3.1. Schematic map and cross section of the units in Eastern Taurides (Özgül, 1976). AD: Aladağ Unit, BD: Bolkardağı Unit, BO: Bozkır Unit, GD: Geyikdağı Unit. Note that the map area comprises part of the Zamantı area.....17
- 3.2. Columnar section of Bolkar Dağı Unit (Özgül, 1976).....18
- 3.3. Columnar section of Aladağ Unit (Özgül, 1976) (see fig. 3.2 for legend).....19
- 3.4. Columnar section of Geyik Dağı Unit (Özgül, 1976) (see fig. 3.2 for legend).....21
- 3.5. Columnar section of Bozkır Unit (Özgül, 1976).....22

3.6. Tectonic units and lead-zinc deposits in Aladağ region , (not to scale) (Ayhan, 1983) (Yahyalı sequence correlates with Bolkardağı unit of Özgül, 1976) .....	24
3.7. Vertical sketch profile of Ağcaşar mine (Çevrim et al., 1986).....	25
3.8. Photograph of hand specimen taken from Aladağ (Zamantı) Zn-Pb mine. Sharp oxidation contact between dark color sulphide (sphalerite+galena and brownish color oxide (smithsonite+cerrusite). Loop diameter is 3 cm as scale.....	25
3.9. Generalized columnar section of Keban area (simplified from Yılmaz et al., 1992).....	29
3.10. Geologic cross-section of the main deposit in Keban area (looking to north) (Köksoy, 1978).....	30
3.11. Generalized geologic map of southeastern Taurus mauntains (Hall, 1976).....	31
3.12. Generalized columnar section of the Bitlis Metamorphic Complex (Göncüoğlu and Turhan, 1997).....	32
3.13. Generalized columnar section of Nigde Massif (Pehlivan et al., 1986).....	34
3.14. Generalized columnar section of Hakkari area (Perincek, 1990).....	37
3.15. Zn- oxide mineralization as matrix of limestone breccia.....	38

4.1. Partial chart of the nuclides. Each square represents a particular nuclide which is defined in terms of the number of protons ( $Z$ ) and neutrons ( $N$ ) that make up its nucleus. The shaded squares represents stable atoms, while the white squares are the unstable or radioactive nuclides (Faure, 1977).....40

4.2. Relative primordial and present-day abundance of the isotopes of uranium (U), thorium (Th), and lead (Pb) showing half-lives in billion of years (Ga). Modifiedd from Cannon et al., (1961) and Gulson (1986) .....43

4.3. Time (Ga) vs cumulative growth (%) of adigenic Pb. Growth of radiogenic Pb with time showing the rapid increase in  $^{207}\text{Pb}^*$  in the early history of the earth because of the relatively short half-life of  $^{235}\text{U}$  (700 m.y.) followed by only limited growth in  $^{207}\text{Pb}^*$  in the last billion years (Ga). The limited growth of  $^{207}\text{Pb}^*$  results from the fact that most  $^{235}\text{U}$  has already decayed, and only a small fraction of the original primordial abundance is still present. Modified from Gariepy and Dupre (1991) .....45

4.4. Thorogenic (A) and Uranogenic (B) Pb isotope diagrams showing the plumbotectonic curves of Zartman and Doe (1981). Thick marks on curves represent 500 million years of growth.....48

4.5. Mixing of multiple Pb sources at the Porgera Au deposit, Papua New Guinea. Modified from Richards et al. (1991). Thorogenic (A) and Uranogenic (B) diagrams show the effect of mixing in the magmatic system (B, trend 1) and in the hydrothermal system (B, trends 2 and 3).....	52
5.1. Positions of Pb-isotope data on uranogenic diagram. S&K (1975): average crustal growth curve of Stacey and Kramers (1975).....	61
5.2. Positions of Pb-isotope data on thorogenic diagram. S&K (1975): average crustal growth curve of Stacey and Kramers (1975).....	62
6.1. Pb-isotope groups on uranogenic diagram. S&K: Average crustal growth curve of Stacey and Kramers (1975), W. Med.: Western Mediterranean growth curve from Aribas & Tosddal (1994), TR: Turkey growth curve from Tosdal (2001).....	66
6.2 Pb-isotope groups on thorogenic diagram. S&K: Average crustal growth curve of Stacey and Kramers (1975), W. Med.: Western Mediterranean growth curve from Aribas & Tosddal (1994), TR: Turkey growth curve from Tosdal (2001).....	67
6.3. Pb-isotope data on uranogenic diagram with the Pb-isotope fields of S. Arabia, France, Spain and Iran are from Bokhari and Kramers (1982), Marcoux and Moelo (1991) and Gilg et al. (2003) respectively. S&K (1975): Average crustal growth curve of Stacey and Kramers (1975).....	73

# CHAPTER 1

## INTRODUCTION

The isotopic composition of lead (Pb) from sulphide minerals provides important constraints on the genesis of ore deposits.

An understanding of the genesis of ore deposits requires to answer the questions addressed to i) sources of ore-bearing fluids and their constituent metals, ii) way of movement of ore-bearing fluids and mechanism of transportation of metals in fluids, iii) mechanism of deposition of metals/minerals from ore-bearing fluids, and iv) the age of mineralization.

Within this framework, Pb-isotope compositions of sulphide minerals (particularly when combined with the compositions of associated rocks) are used to i) determine the source of Pb (and other metals) in ore deposits, ii) investigate the nature of interaction between ore-bearing fluids and the wall rocks, iii) assess the role of regional controls (tectonic setting, influence of basement rocks) on mineralization, and iv) provide chronological information (absolute or relative) for formation of ore deposits.

This thesis study is concerned with the Pb-isotope composition of galena minerals collected from the Pb-Zn occurrences in southern Turkey. The majority of the investigated occurrences are located within one of the major tectonic units of Turkey, the Taurides, although few occurrences out of this tectonic unit (one is in the Arabian Platform and the other in the Central Anatolian Crystalline Complex) are also examined in this context.

### 1.1. Purpose and Scope

This study is aimed to contribute to the understanding of the genesis of Pb-Zn occurrences in southern Turkey through the use of Pb-isotope composition of sulphide minerals. The purpose is of 3-folds: i) to investigate the source(s) of lead in the occurrences, ii) to provide chronologic information for formation of ore

deposits and iii) to examine the possible control, on the Pb-isotope composition, of tectonic setting and crustal basement, the latter referring to the basement as well as the crustal column traversed by hydrothermal solutions. Within this framework, the Pb-isotope database established by Teck Cominco Madencilik San. A.S. is used. The database covers the  $^{206}\text{Pb}/^{204}\text{Pb}$ ,  $^{207}\text{Pb}/^{204}\text{Pb}$  and  $^{208}\text{Pb}/^{204}\text{Pb}$  ratios of a total of 43 galena samples collected from several Pb-Zn occurrences located essentially in Eastern Taurides (Zamantı, Kahramanmaraş (K. Maraş), Malatya, Keban-Elazığ and Zizan-Bitlis areas), with some additional data from Niğde and Hakkari areas.

## **1.2. Methods of Study**

The galena samples used in the establishment of the Pb-isotope database have been collected by Teck Cominco Madencilik San. A.S. geologists since 2000 and analysed in the laboratories (e.g. Geospec Consultants Limited) in Canada. The Pb-Isotope data interpretation is made using Uranogenic and Thorogenic diagrams, in the light of i) the available information relevant to the geology of the areas and mineralization type of the Pb-Zn occurrences, ii) field observations. As a field geologist in the same company, I have worked in most of the studied areas like Zamantı, Keban and Hakkari, and carried out prospecting and geological mapping.

## **1.3. Geographic Setting**

The Pb-Zn occurrences studied in this thesis are located in 7 different areas, namely, Niğde, Zamantı (Kayseri, Adana), K. Maraş, Malatya, Elazığ, Bitlis and Hakkari. The geographic setting of these areas are shown in Figure 1.1. The areas are included in the following (1/100 000 scale) topographic maps of Turkey: Niğde (M 33), Zamantı (M 34, L34-35-36), K. Maraş (L37, M 38), Malatya (L 39-40), Elazığ (K 41), Bitlis (L 47) and Hakkari (N 50-51) (Appendix A).

#### **1.4. Layout of Thesis**

This thesis contains 7 chapters. Following this introduction chapter, an overview of the tectonic setting and regional geology of the studied areas is given in Chapter 2; an outline of the geology and mineralization in the studied areas is presented in Chapter 3; background information about the Pb-isotopes and their use in ore genesis is provided in Chapter 4; Pb-isotope data pertinent to the studied occurrences are presented in Chapter 5; discussion of the Pb-isotope data is made in Chapter 6 in terms of possible implications as to the age and source of mineralization together with an evaluation of the possible effects of tectonic setting and the crustal basement; Chapter 7 summarizes the conclusions reached in this study.

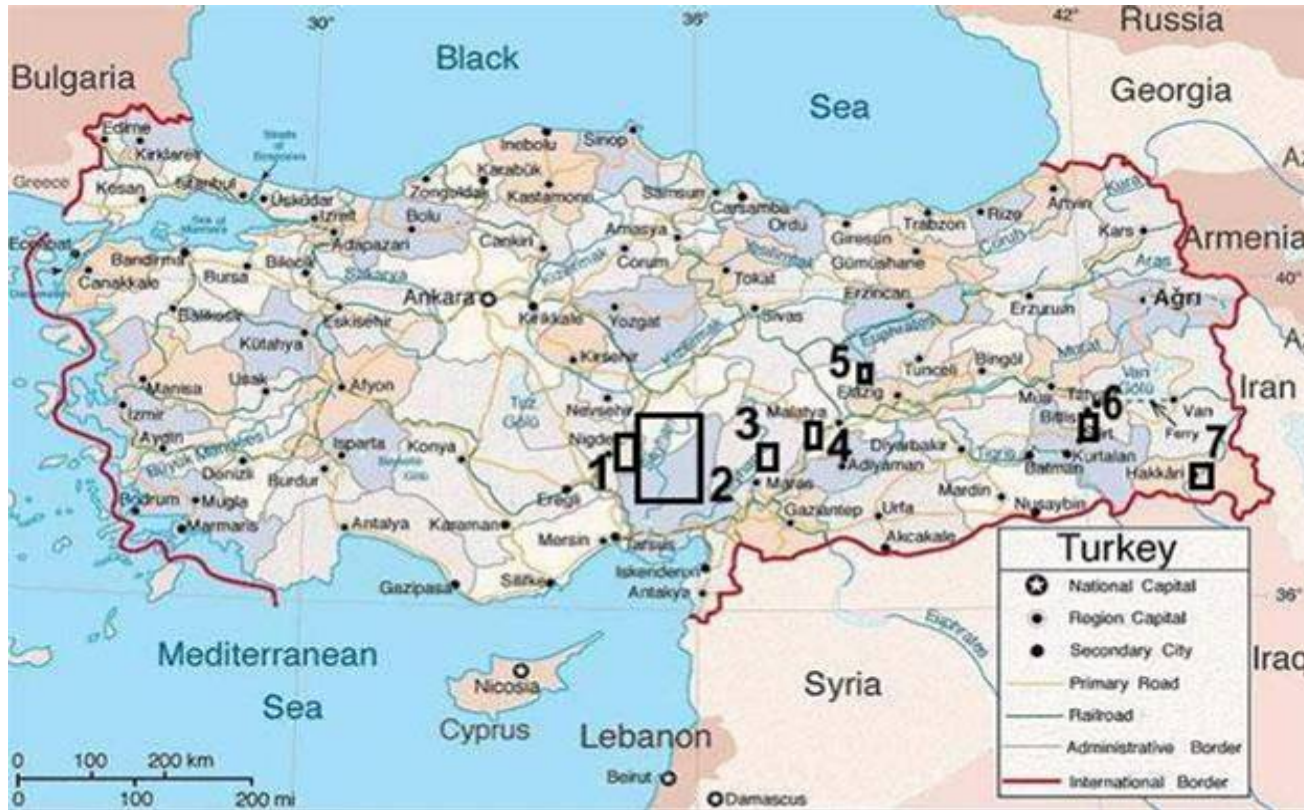


**Figure 1.1.** Location map of the studied areas (1.Niğde area, 2. Zamantı area, 3. K. Maraş area, 4. Malatya area, 5. Elazığ are, 6. Bitlis area, 7. Hakkari area).

## CHAPTER 2

### TECTONIC SETTING AND REGIONAL GEOLOGY

Turkey, currently forming an important segment of the Alpine-Mediterranean Belt, was once located at the boundary of two megacontinents: Gondwana in the south and Laurasia in the north. The present geological framework of Turkey was established during the Alpine orogeny caused by the collision of the African and the Arabian plates in Late-Cretaceous-Tertiary time. This orogeny was associated with the separation, rotation, collision and deformation of many small continental fragments which are now bounded by various suture zones developed as a result of the closure of several branches of the Neotethys (Şengör and Yılmaz, 1981; Okay, 1986; Bozkurt and Mittweide, 2001).

In early years, Turkey is divided into four major tectonic units (from N to S): Pontides, Anatolides, Taurides and Border Folds (Ketin, 1966). This was followed by different subdivisions proposed by different authors (e.g. Şengör and Yılmaz, 1981; Okay, 1986; Okay and Tüysüz, 1999; Göncüoğlu et al., 2000). Most recently, Bozkurt and Mittweide (2001) synthesized previous studies related with geology of Turkey. This thesis study uses the tectonic subdivisions (Fig 2.1) adopted from Bozkurt and Mittweide (2001), that is essentially based on the scheme recently proposed by Okay and Tüysüz (1999). According to this scheme, Turkey is traversed by five major Neotethyan suture zones: İzmir-Ankara-Erzincan, Intra-Pontide, Inner Tauride, Antalya and Southeast Anatolian. These suture zones form the boundaries of the microcontinental fragments (Fig 2.1) which are from north to south:

- Pontides: comprises three major tectonic zones: i) Strandja ii) İstanbul iii) Sakarya (as is formerly proposed by Okay, 1986)
- Tauride-Anatolide Platform (TAP) (Şengör and Yılmaz, 1981): Taurides and Anatolides of Ketin (1966) are treated together. Anatolides, representing the metamorphic northern margin of the Tauride-Anatolide platform, comprises the zones namely: i) Bornova Flysch, ii) Tavşanlı



zone, iii) Afyon zone, iv) Menderes Massif (MM) and Central Anatolian Crystalline Complex (CACC: Göncüoğlu et al., 1991) which is also known as Kırşehir Massif (Seymen, 1981).

- Arabian Platform: corresponds to the Border Folds of Ketin (1966)

Within the framework of this classification, the studied areas in this thesis are located in:

- Taurides (including Zamantı, K. Maraş, Malatya, Keban-Elazığ and Bitlis areas)
- southeastern edge of Kırşehir Massif (known as Niğde Massif) (including Niğde area).
- Arabian Platform (including Hakkari area)

Taurides is composed of a pre-Cambrian basement and non-metamorphic and/or slightly metamorphosed Cambrian to Tertiary rock units (Özgül, 1976, 1985; Okay and Özgül, 1984; Okay, 1989). Özgül (1976) who studied the geology of the Taurus mountains differentiated several rock units based on their stratigraphic position, character of metamorphism and present structural position. These units (from N to S) are named as Bozkır Unit, Bolkar Dağı Unit, Aladağ Unit, Geyikdağı Unit, Antalya Unit, and Alanya Unit (Fig. 2.2). All these units have tectonic contacts and form allocthonous covers on each other. Bolkardağı, Aladağ, Geyikdağı and Alanya units mainly consist of shelf type carbonates and detrital rocks. On the other hand, the Bozkır and Antalya units contain deep sea sediments, ophiolites and submarine basic volcanic rocks.

Central Anatolian Crystalline Complex (CACC) comprises Kırşehir Massif at the north, and Niğde Massif at the south. CACC consists of Paleozoic-Mesozoic aged medium to high grade metamorphics (marbles, gneises, schists, amphibolites), Mesozoic ophiolitic rocks representing remnants of Neo-Tethyan ocean floor, and voluminous Cretaceous granitoids with minor mafic intrusions (Seymen, 1981; Göncüoğlu, 1986; Göncüoğlu et al., 1991; Akıman et al., 1993; Güleç, 1994; Yalınız et al., 1999; Whitney D. L. et al., 2001; Kadıoğlu et al., 2003) (Fig. 2.3).

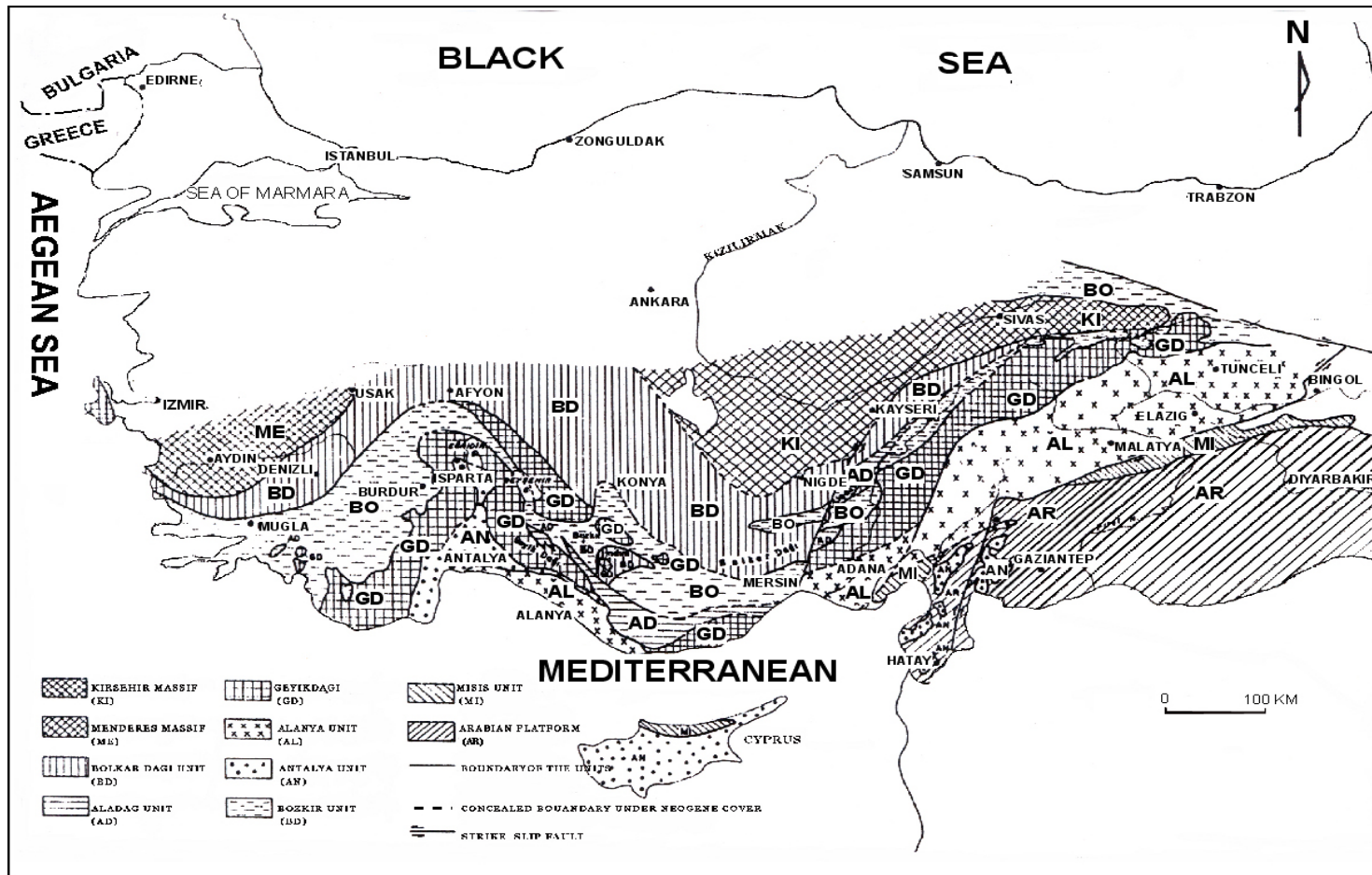


Figure 2.2. Geologic map showing the distribution of units in Taurides (Özgül, 1976)

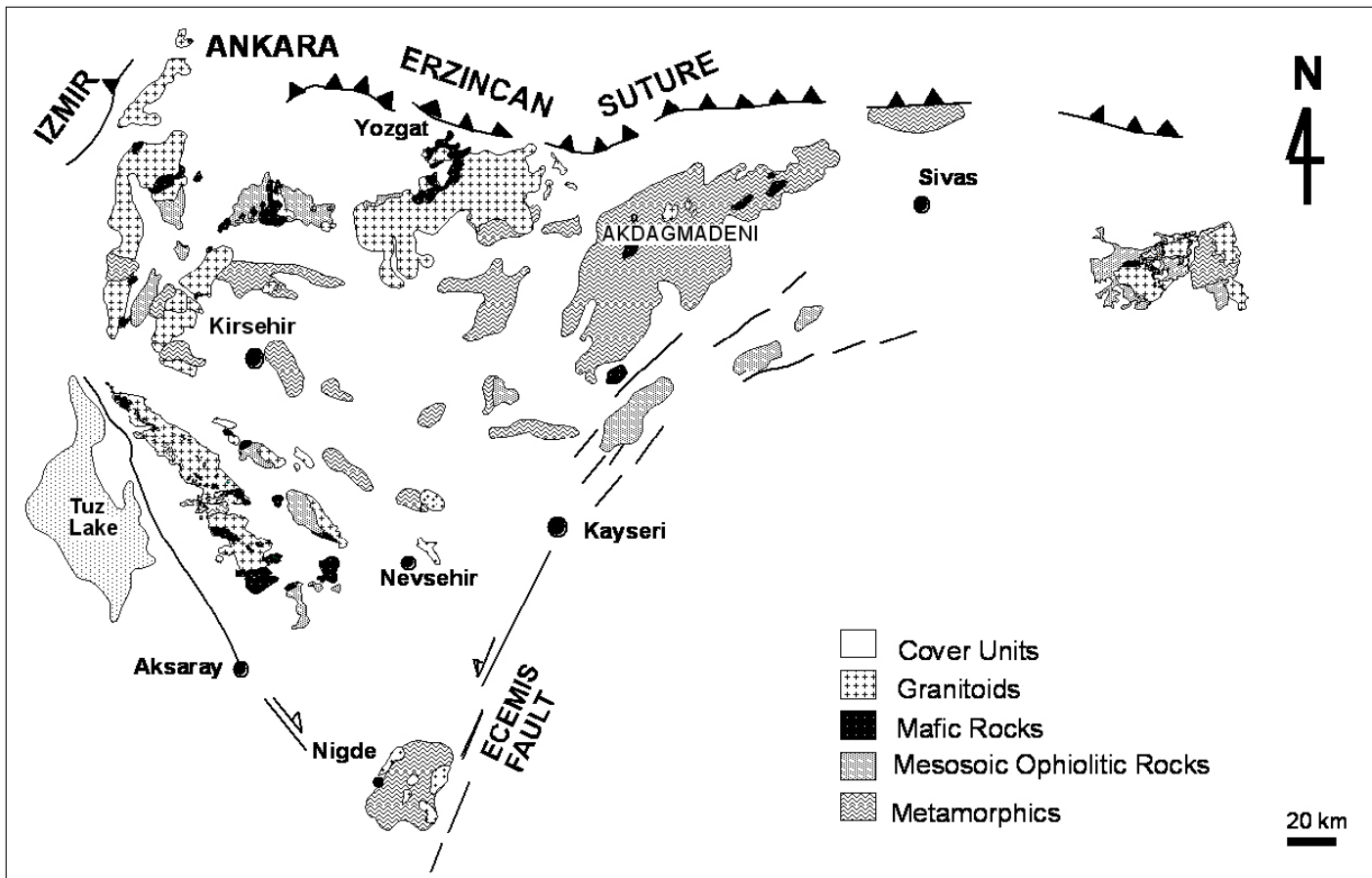


Figure 2.3. Geologic map of Central Anatolian Crystalline Complex (Kadioglu et al., 2003)

Göncüoğlu (1986) suggest Pre- Late Cretaceous age for the main stage of metamorphism in CACC.

Arabian Platform mainly consists of a Pan-African basement and its Paleozoic-Tertiary cover. The platform includes a mostly marine, sedimentary succession of about 10-km- thick which ranges in age from Early Cambrian to Middle Miocene (Yılmaz, 1993). The deposition up to Early Cretaceous is characterized by platformal carbonates. The Alpine cycle in the platform commenced with the Middle Triassic rifting (Altiner, 1989) and followed by compressional forces originated from different directions during the Late Cretaceous and Late Miocene times (Perinçek 1990).

# CHAPTER 3

## OUTLINE OF GEOLOGY AND MINERALIZATION IN THE STUDIED AREAS

### 3.1. Introduction

The studied areas are mainly located in three different tectonic units, namely, Taurides, CACC and Arabian Platform.

Zamantı, K. Maraş-Afşin, Malatya, Keban and Bitlis areas studied in this thesis are all located within the Tauride Belt. Zamantı area is located on the western edge of the Eastern Taurides and limited by Ecemiş Fault in the west, Kayseri city in the north, K. Maraş city in the east and Adana city in the south. K. Maraş-Afşin, Malatya and Keban areas are located in the central part, whereas Bitlis area is located on the eastern edge (in the well-known Bitlis Massif) of the Eastern Taurides.

Niğde area is located within the Niğde Massif which forms an integral part of CACC. The mineralization in the Hakkari area is located within the Arabian Platform.

The information relevant to the geologic outline of, and the mineralization in the studied areas is summarized in Table 3.1.

The Pb-Zn mineralizations in the studied areas comprise mainly non-sulphide minerals (e.g. smithsonite, hydrozincite) with minor sulfide (e.g. galena) occurrence

Table 3.1. The information relevant to the geologic outline of, and the mineralization in the studied areas with UTM coordinates of samples (Lmst: limestone, CRD: Carbonate replacement deposits, MVT: Mississippi Valley type).

Number	UTM Zone (S)	Easting	Northing	Location	Host Rock	Age of host rock	Mineralization in Field Observation
1	36	669033	4189283	Niğde - Celaller	Schist - Marble	pre-Cretaceous	Skarn + CRD
2	36	672600	4194250	Niğde	Marble	pre-Cretaceous	Skarn + CRD
3	36	695948	4224023	Kayseri-(S of <i>Çadırkaya Fe deposit</i> )	Lmst and andesite	Permian	Skarn
4	36	695667	4223847	Kayseri-(S of <i>Çadırkaya Fe deposit</i> )	Lmst and andesite	Permian	Skarn
5	36	689763	4224860	Kayseri (2 km SW of Ismail Inkaya Fe deposit)	Lmst	Permian	Skarn
6	36	730974	4228934	Kayseri ( near Yoncaliseki Zn-Pb-Fe showing)	Lmst	Late Cretaceous	CRD
7	36	707745	4230174	Kayseri-Kocahacılı	Lmst	Permo-Carboniferous	Stockwork
8	36	721400	4226000	Kayseri-( <i>Denizovası-Kızıltepe-Demirtepe Zn-Pb deposit</i> )	Lmst	Carboniferous-Late Permian	Karstic filling along fault zone
9	36	718850	4225080	Kayseri-(W of <i>Denizovası</i> )	Lmst	Devonian	CRD

Table 3.1. The information relevant to the geologic outline of, and the mineralization in the studied areas with UTM coordinates of samples (Lmst: limestone, CRD: Carbonate replacement deposits, MVT: Mississippi Valley type) (continued).

10	36	701007	4201099	Kayseri-(Near <i>Aladağ-Delikkaya Pb-Zn deposit</i> )	Lmst	Late Devonian-Jurassic	CRD
11	36	701300	4201600	Kayseri-(Near <i>Aladağ-Delikkaya Pb-Zn deposit</i> )	Lmst	Late Devonian-Jurassic	CRD
12	36	698130	4200127	Kayseri-( <i>Aladağ-Delikkaya Pb-Zn deposit</i> )	Lmst	Late Devonian-Jurassic	Stockwork vein
13	36	699315	4200823	Kayseri-( <i>Aladağ-Delikkaya Pb-Zn deposit</i> )	Lmst	Late Devonian-Jurassic	Stockwork vein
14	36	719448	4225884	Kayseri-( <i>Ayoluğu Zn-Pb deposit</i> )	Lmst	Jurassic- Late Cretaceous	Karstic filling along fault zone
15	36	694524	4216441	Kayseri-( <i>Dünderli Pb-Zn deposit</i> )	Lmst	Devonian-Cretaceous	Fracture and karstic filling
16	36	706923	4206272	Kayseri-( <i>Suçatı Pb-Zn deposit</i> )	Lmst	Jurassic	Fracture and karstic filling
17	36	755831	4227895	Kayseri-( <i>Saraycık Pb-Zn deposit</i> )	Lmst	Devonian	Fracture filling conformable with bedding

Table 3.1. The information relevant to the geologic outline of, and the mineralization in the studied areas with UTM coordinates of samples (Lmst: limestone, CRD: Carbonate replacement deposits, MVT: Mississippi Valley type) (continued).

18	36	726008	4226173	Kayseri-(Çakılıpınar Zn-Pb deposit)	Lmst-dolomite	Jurassic-Late Cretaceous	Vein
19	36	699841	4219076	Kayseri-(Dereköy-Ayraklı Zn-Pb deposit ' <i>Oreks'</i> )	Lmst-schist contact and lmsst	Devonian	Fracture filling
20	36	699841	4219076	Kayseri-(Dereköy-Ayraklı Zn-Pb deposit ' <i>Oreks'</i> )	Lmst-schist contact and lmsst	Devonian	Fracture filling
21	36	722001	4226727	Kayseri-(Celaldağı Zn-Pb deposit)	lmsst	Late Permian	Along fault zone
22	36	716268	4213132	Kayseri- <i>Ayvan (Sultankuyu Fe Showing)</i>	Lmst	Carboniferous	Karstic filling
23	36	738879	4219785	Kayseri-(Kaleköy Zn-Pb deposit)	Dolomite	Devonian	Vein
24	36	712400	4226000	Kayseri-(Ağcaşar Zn-Pb-Fe deposit)	Lmst	Triassic	Strata bound
25	37	268666	4231456	Adana-Tufanbeyli-Bozcal	Dolomite	Devonian	MVT
26	37	265644	4220990	Adana-Tufanbeyli-Akçal	Dolomite	Devonian	MVT
27	37	264273	4242040	Adana-Tufanbeyli	Dolomite	Devonian	Vein
28	37	318652	4226580	K.Maraş-Afşin	Andesite	Late Cretaceous	Vein
29	37	317883	4232345	K.Maraş-Afşin	Granite	Tertiary	Disseminated
30	37	314240	4231930	K.Maraş-Afşin	Ophiolite		As galena pods

Table 3.1. The information relevant to the geologic outline of, and the mineralization in the studied areas with UTM coordinates of samples (Lmst: limestone, CRD: Carbonate replacement deposits, MVT: Mississippi Valley type) (continued).

31	37	301200	4234170	K.Maraş-Afşin- <i>Türksevin</i>	Lmst	Permo-Carboniferous	Vein
32	37	329285	4184286	K.Maraş-Engizek- <i>Çiğdem</i>	Lmst	Miocene	Vein
33	37	328622	4184328	K.Maraş-Engizek- <i>Çal</i>	Lmst	Miocene	Veins along fractures
34	37	403181	4228245	Malatya-Adatepe	Lmst	Permo-Carboniferous	CRD
35	37	425000	4237000	Malatya-Cafana	Lmst	Permo-Carboniferous	CRD
36	37	419600	4218600	Malatya-Cafana-Melet deresi	Marble	Paleozoic	CRD
37	37	475978	4297112	Elazığ- Keban	Marble, lmsst, dolomite	Devonian	Skarn + vein
38	37	759181	4239310	Bitlis-Zizan-Dava	Lmst , Marble	Permian	Vein
39	37	759166	4239454	Bitlis- Lower Zizan	Lmst	Permian	Vein
40	38	SW of	Hakkari	Hakkari	Lmst	Jurassic-Cretaceous	Stratabound
41	38	SW of	Hakkari	Hakkari	Lmst	Jurassic-Cretaceous	Stratabound
42	38	SW of	Hakkari	Hakkari	Lmst	Jurassic-Cretaceous	Stratabound
43	38	SW of	Hakkari	Hakkari	Lmst	Jurassic-Cretaceous	Stratabound

## 3.2. Studied Areas in Taurides

### 3.2.1. Zamantı Area

#### 3.2.1.1. *Geologic Outline*

First studies related with the general geology of the area (Tschihatscheff, 1869; Schaffer, 1903; Frech 1916; Philippson 1918; Metz, 1939) were summarized by Blumenthal in 1952. Özgül (1976) studied the Taurus mountains and differentiated the units by their stratigraphic position, degree of metamorphism and their present structural position. Other geological studies about the region were undertaken by Tekeli (1980, 1981), and Tekeli et al. (1981).

In the Zamantı area, most of the Pb-Zn deposits are located near Yahyalı village. Bolkardağı, Aladağ, Geyikdağı and Bozkır units extend laterally for tens of kilometers without losing their characteristics in the area (Fig. 3.1). The characteristics of the units (as taken from Özgül, 1976) are as follows:

#### Bolkardağı Unit

This unit extends from west of Milas in the west, through Denizli, Afyon, Konya and Bolkardağı, to Niğde in the east. The Bolkardağı unit contains Middle Devonian to Lower Tertiary rock units (typically shelf type carbonates and clastic rocks in Devonian-Upper Cretaceous, and olistoliths in Maastrichtian-Paleocene) (Fig 3.2). The unit shows metamorphism in mostly green schist facies.

#### Aladağ Unit

The name of the unit is from one of the highest mountains, Aladağ, located in Middle Taurides (Fig. 3.3). The unit is composed of the rock units deposited during Late Devonian-Maastrichtian time. Late Devonian-Late Cretaceous interval is dominantly characterized by the deposition of shelf type carbonates and clastic rocks. During Late Paleozoic and Mesozoic, except for the beginning of Late Triassic, continuous deposition exists. Upper Triassic is represented by almost 500 m thick conglomerates. No metamorphism is observable in the unit.

Biozones of Carboniferous and Lower Permian are well developed and extend laterally hundreds of kilometres. Algs of Permian age are well developed. The unit is allocthonous with respect to the other units in all the areas where observable.

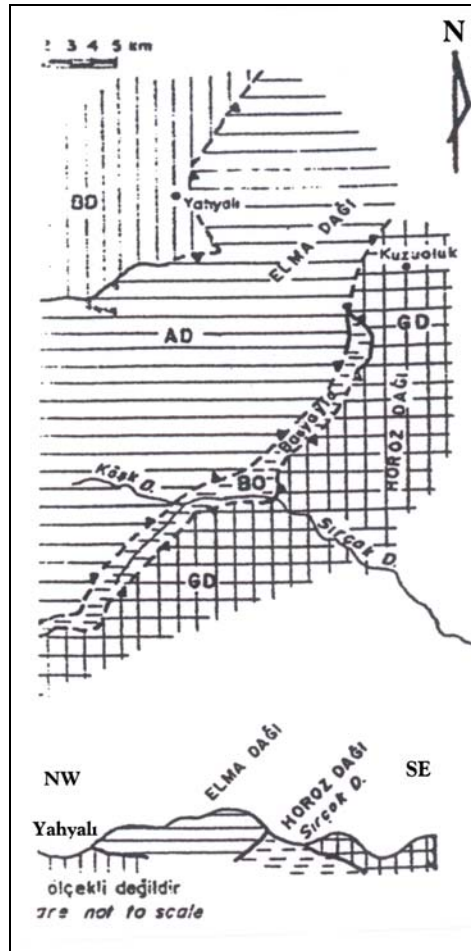


Figure 3.1. Schematic map and cross section of the units in the Eastern Taurides (Özgül, 1976). AD: Aladağ unit, BD: Bolkardağı unit, BO: Bozkır unit, GD: Geyikdağı unit. Note that the map area comprises part of the Zamanti area.

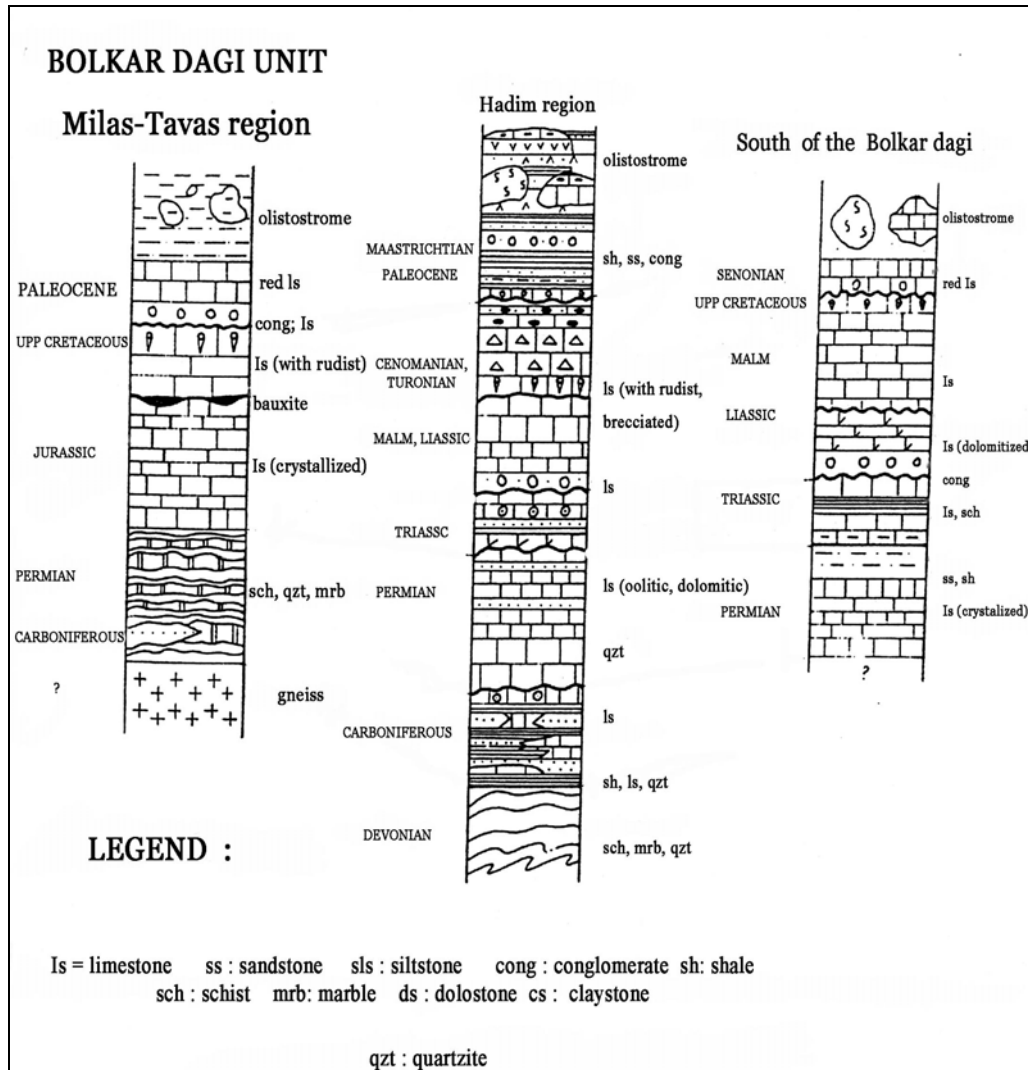


Figure 3.2. Columnar section of Bolkar Dağı Unit (Özgül, 1976)

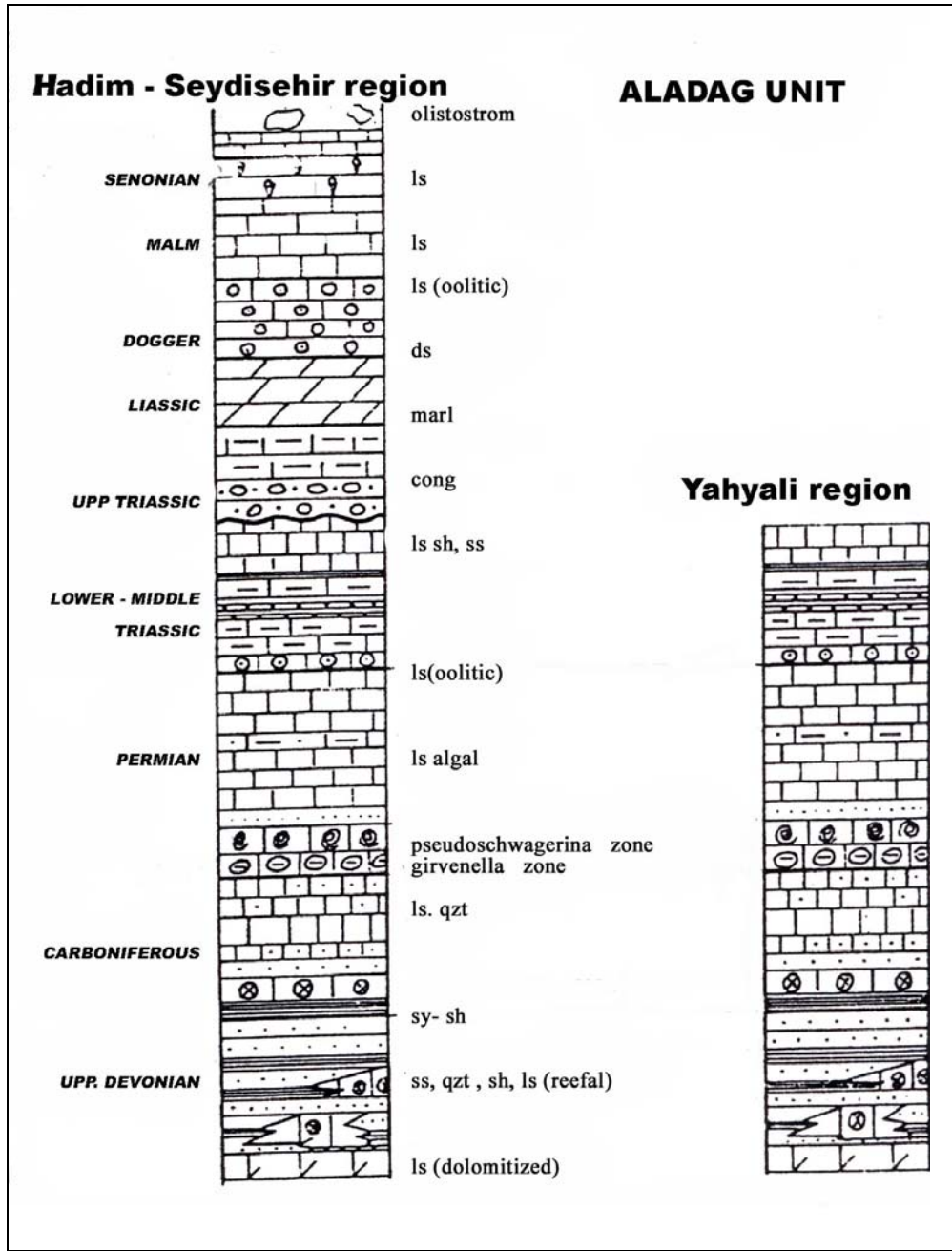


Figure 3.3. Columnar section of Aladağ Unit (Özgül, 1976) (see fig. 3.2 for legend).

### Geyikdağı Unit

The unit is autochthonous with respect to Aladağ and Bolkardağı units in the Zamantı area. It consists of Cambrian-Tertiary rock units. Paleozoic is represented mainly by clastic rocks and Mesozoic platformal carbonates (Fig. 3.4). No metamorphism is observable in the unit.

### Bozkır Unit

The unit is made up of several rock units of different ages and consists of radiolarites and pelagic limestone with chert, ophiolite blocks of various sizes, tuffs, basic submarine volcanic rocks, and conglomerate blocks with several kilometers in diameter (Fig 3.5). The unit comprises the Maastrichtian-Lutetian olistostrome of Bolkardağı, Aladağ, and Geyikdağı units.

### Yahyalı/Karamadazı Granitoids

The Yahyalı/Karamadazı igneous rock consists of granite, granodiorite, quartz-diorite, and diorite. According to Ayhan (1983) it is post-Cretaceous but older than Early Eocene in age. Ages such as Hersinian (Ulakoğlu, 1983) and Eocene-Oligocene (Oygür, 1986) were also suggested for the unit. The unit can be observed in a limited area in Zamantı region.

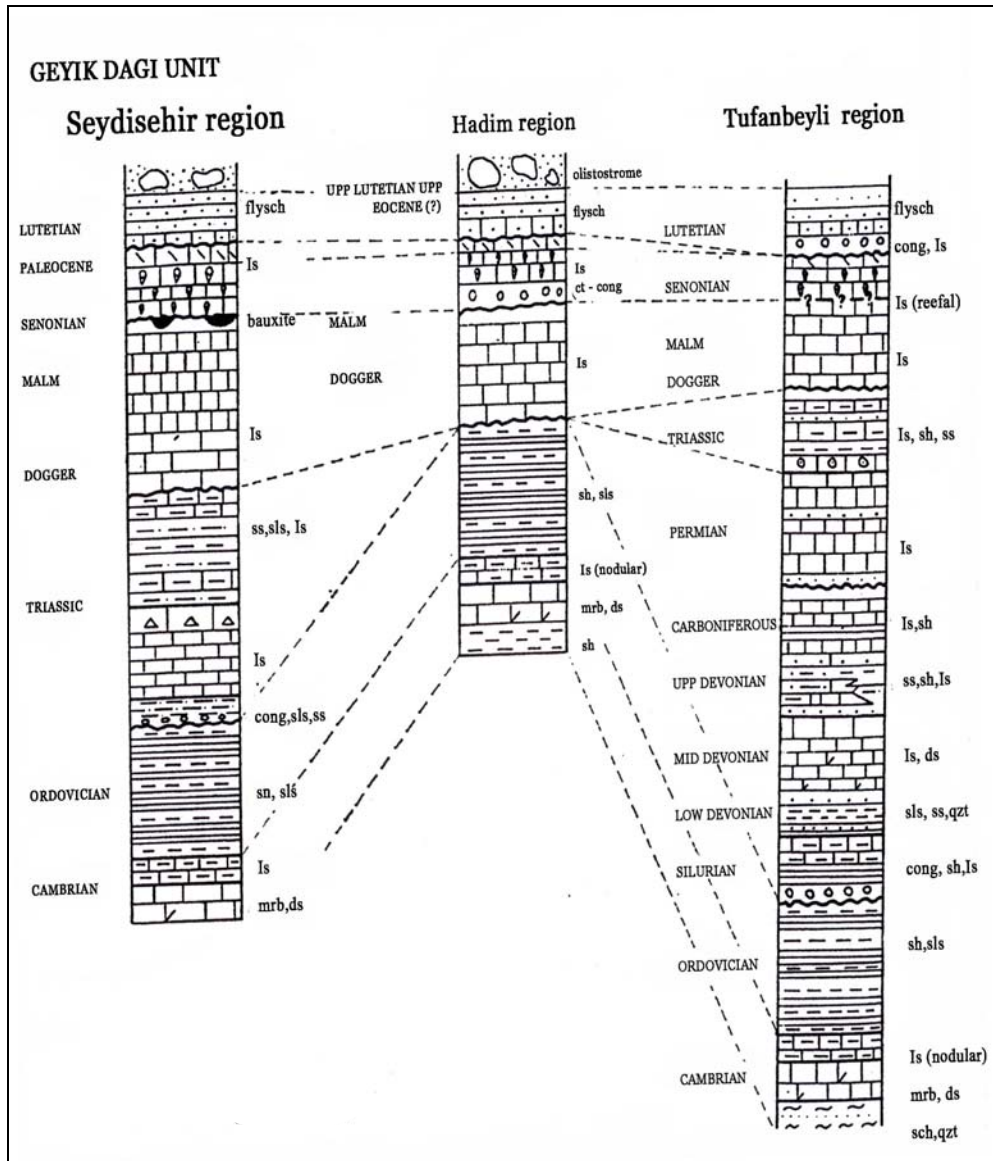


Figure 3.4. Columnar section of Geyik Dağı Unit (Özgül, 1976) (see fig. 3.2 for legend).

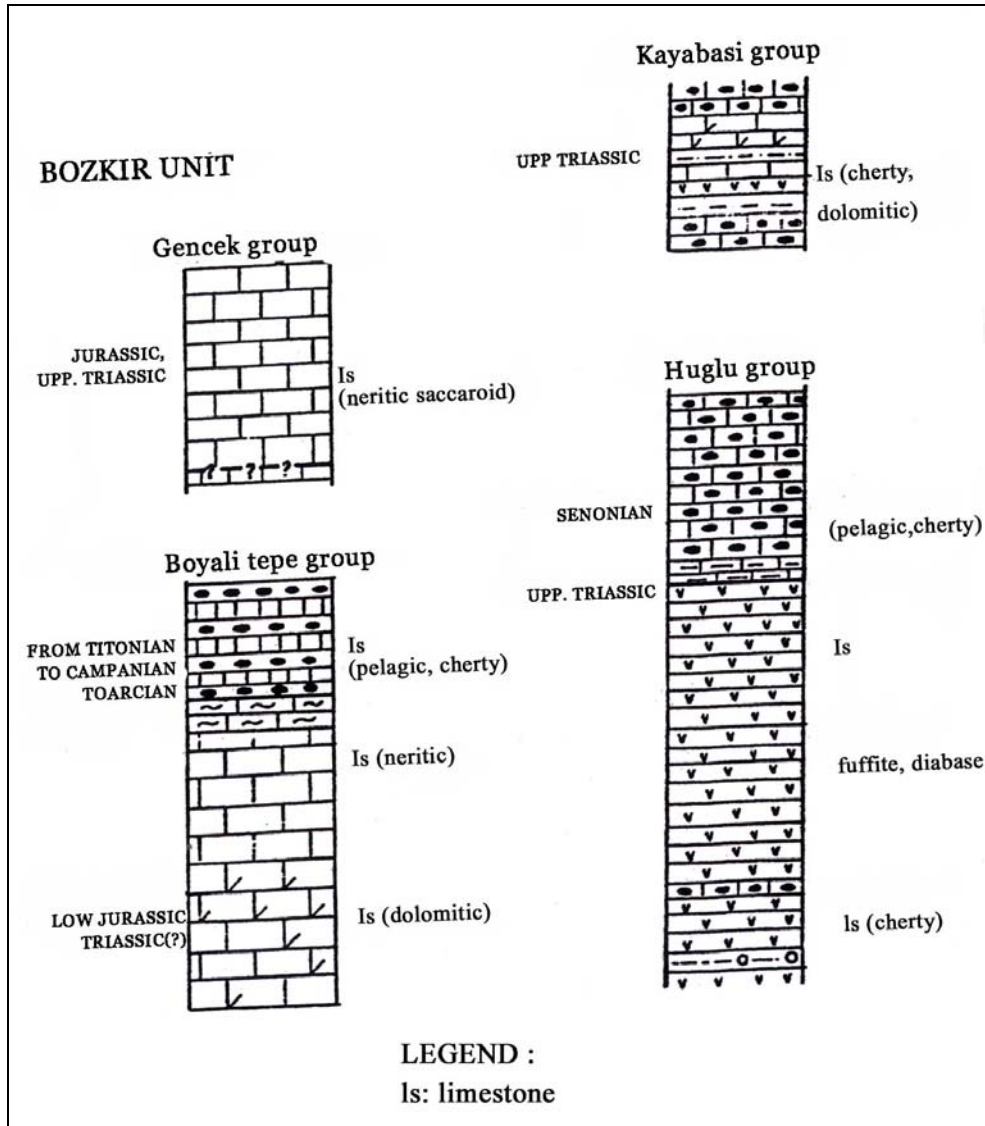


Figure 3.5. Columnar section of Bozkır Unit (Özgül, 1976).

### ***3.2.1.2. Mineralization***

There are a number of Pb-Zn occurrences in the Zamantı area. The mineralizations are mainly hosted by Devonian – Upper Cretaceous carbonates. The ore minerals in these occurrences were deposited as fillings of karstic networks in fracture zones. The mineralized material consists, in general, of chemically or mechanically transported fragments. Replacement of the wall rock represents an important process of mineralization only in structure-controlled weakness zones in massive limestones. The sulfide paragenesis consisting almost entirely of sphalerite, galenite and pyrite/marcasite, is rare in all occurrences due to oxidation processes. The oxidic ores contain predominantly smithsonite, hemimorphite, hydrozincite, Zn-Al-silicates and high amounts of limonite. The filling-type ores occurring in layers and/or as cement of clastic sediments reveal very heterogenous composition and structures with characteristic variations in different karst zones (Çevrim et al., 1986)

Ayhan (1983) in his study summarized previous works about the deposits in the Zamantı Region. One of these previous works belongs to Vache (1964, 1966) who described some deposits (e.g., Kaleköy) in the western and central Zamantı as SEDEX-type deposits formed in a sedimentary environment. According to Vache (1966), the mineralization is of Permian age and the ore bodies have different shapes like lenses, layers and veins. According to Imreh (1965) and Wohryzka (1966), Zamantı deposits are magmatic-related hydrothermal-karstic filling ore deposits. Metag and Stolberg (1971), in their study concerned with the economic potential of the deposits, related the genesis of the deposits to hydrothermal-metasomatic processes. According to Ayhan (1983), ore solutions of Zamantı, which are related to Yahyalı/Karamadazı granitoids, could have reached Aladağ ophiolitic melange (Bozkır Unit of Özgül, 1976) and mineralized all units throughout its way. After their deposition, the sulphide-bearing ore minerals were altered to carbonate-bearing minerals by the multikarstification processes during and after the uplifting of the region (Fig. 3.6).

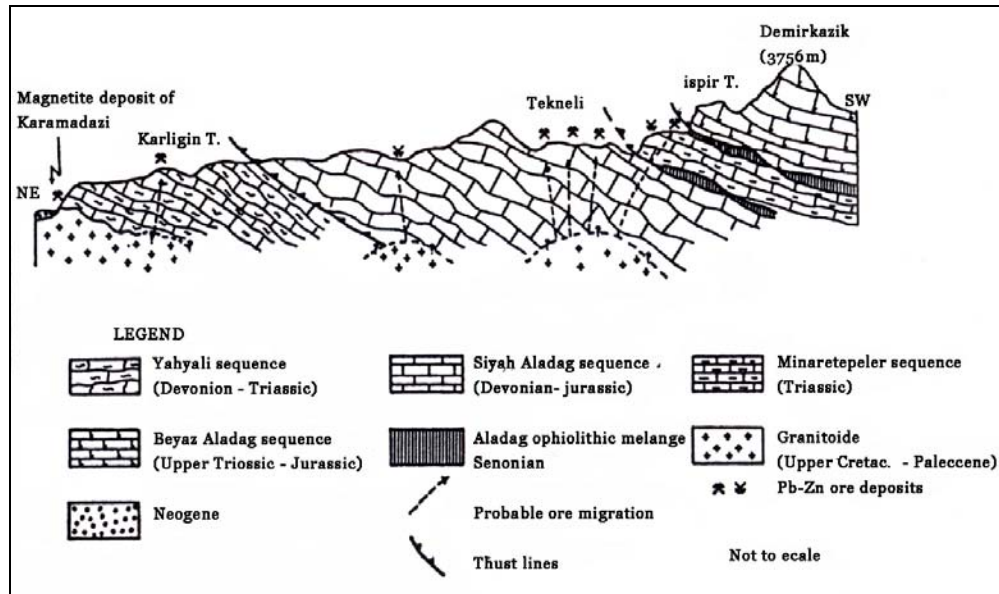


Figure 3.6. Tectonic units and lead-zinc deposits in Aladağ region (not to scale) (Ayhan, 1983) (Yahyali sequence correlates with Bolkardağı unit of Özgül, 1976)

According to Çevrim et al. (1986), the mineralization depends neither on the stratigraphy of the host rock nor on any magmatic activity. The occurrences are hosted by palaeokarst features, developed at the post Cretaceous emergence surfaces in Permian and Jurassic limestone series. The distribution and shape of the ore deposits are influenced by the local fracturing and paleokarstification related to the varying lithology (Fig. 3.7).

According to Lengeranlı (1982-1983), Pb-Zn occurrences in the region are hosted by the rock units ranging from Ordovician to Cretaceous in age. Wall rocks are dolomite and limestones and the deposits are karst-filling type.

Both sulphide and oxide ore minerals can be seen in most of the occurrences (Fig. 3.8)

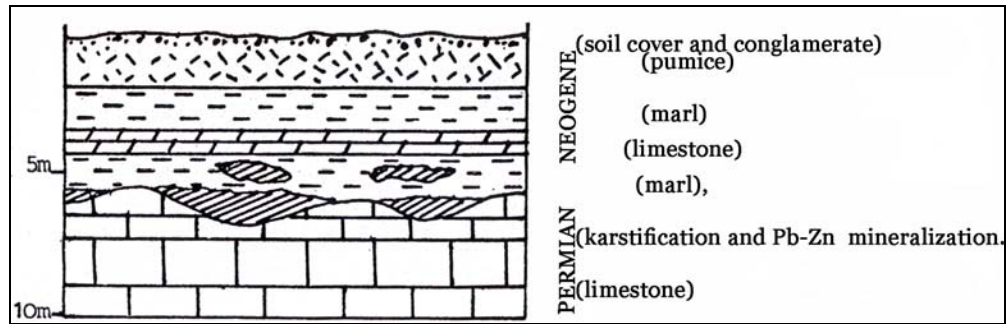


Figure 3.7. Vertical sketch profile of Ağcaşar mine (Çevrim et al., 1986)

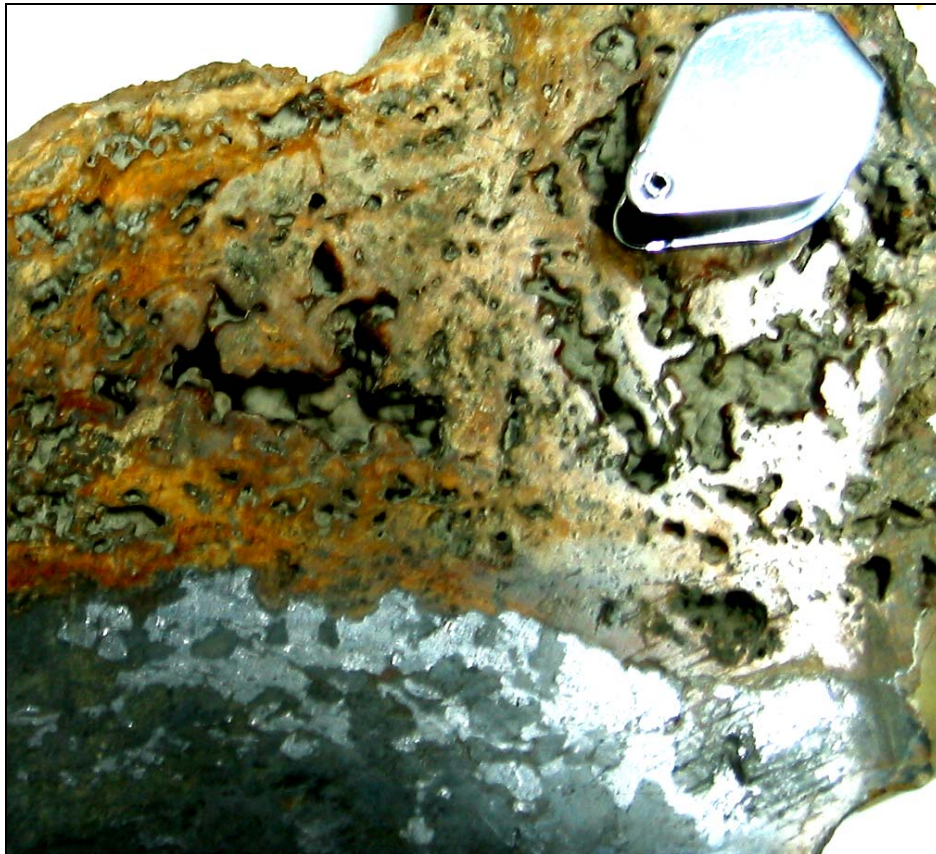


Figure 3.8. Hand specimen taken from Aladağ (Zamantı) Zn-Pb mine. Sharp oxidation contact between dark color sulphide (sphalerite+galena) and brownish color oxide (smithsonite+cerrusite). Loop diameter is 3 cm as scale.

### **3.2.2. K. Maraş Area (Afşin, Türksevin, Engizek)**

#### ***3.2.2.1. Geologic Outline***

K. Maraş-Afşin occurrences are located in the Alanya Unit of Özgül (1976). Although the Alanya Unit is described by Özgül (1976) as consisting of Permian-Lower Tertiary metamorphic rocks in Alanya area, in the eastern extension of the unit through K. Maraş to Tunceli, granitic, andesitic, ophiolitic rocks and limestones together with metamorphics are observed as host rocks of the Pb-Zn mineralizations.

Adıgüzel et al. (1991) in their study on the northern part of K. Maraş region, distinguished two units in Paleozoic metamorphic basement: Kapaktepe (gneiss, schist and marble) and Çağılhan metamorphics (schists), the latter overlying the former with an unconformity. The metamorphics are unconformably overlain by Jurassic-Cretaceous Andırın limestone. Upper Jurassic-Lower Cretaceous Göksün Ophiolites comes over the metamorphics and Andırın limestones with a tectonic contact. Both metamorphics and ophiolites are cut by granitic intrusions (Tarhan, 1986). Maastrixtian-Tertiary sedimentary formations (Ercene, Fındık and Salyan formations) consist mainly of clastic rocks and carbonates. Quaternary alluvium form the youngest unit in the region.

#### ***3.2.2.2. Mineralization***

The Afşin-Türksevin mineralization is hosted by quartz-sericite schist and by crystalline limestone. The field observations by Teck Cominco geologists suggest the presence of vein-type mineralization in Afşin-Türksevin area.

Engizek mineralizations (Çal and Çiğdem occurrences) are hosted by Miocene limestones where sphalerite and galena can be observed as veins along fractures.

The presence of three other occurrences in the Afşin area is reported by Teck Cominco geologists. These occurrences are hosted by Upper Cretaceous andesite, Tertiary granite and ophiolites (see Table 3.1). In granite hosted deposits,

mineralization is observed as disseminations, whereas in ophiolite hosted ones, mineralization is in the form of galena pods.

### **3.2.3. Malatya Area ( Cafana, Adatepe)**

#### ***3.2.3.1. Geologic Outline***

The area is located in Eastern Taurides, in the Alanya Unit of Özgül (1976). The geodynamic evolution of the E Taurides involving an arc-continent collision between the Keban microplate and Arabian plate during late Campanian-early Maastrichtian in the region of Malatya. The Zn-Pb mineralizations in the area occur within the fault zones cutting the Permo-Carboniferous Malatya metamorphics (Önal et al., 1990). The metamorphics consist of limestones and marbles (Cengiz et al., 1991), intercalated with schists (Önal et al., 1990; Sağıroğlu, 1988). The metamorphics are overlain by volcano-sedimentary units which are cut by andesitic volcanic rocks (Önal et al., 1990; Cengiz et al., 1991). Quaternary alluvium and slope materials comprises the youngest unit in the area.

#### ***3.2.3.2 Mineralization***

There are two main occurrences in the area: Cafana and Adatepe. The Adatepe mineralization is hosted by Carboniferous limestone, whereas Cafana mineralization is observed in andesitic volcanics and along the contact of these volcanics with Malatya Metamorphics and the volcanosedimentary units. Önal et al. (1990) and Cengiz et al. (1991) suggested hydrothermal source-related with andesitic (Paleocene in age: Önal et al., 1990) volcanics for Cafana mineralization. The major ore minerals are smithsonite, galena and sphalerite. According to Sağıroğlu (1988), sphalerite and galena comprise the early minerals of the paragenesis in Cafana mineralization, while smithsonite represents the alteration product of sphalerite.

### **3.2.4. Keban Area**

#### ***3.2.4.1. Geologic Outline***

The area is located in Eastern Taurides, within the Alanya Unit of Özgül (1976). The Keban area, in general, shows a simple synclinal basin-like structure, extending 7 km north-south and 3 km east-west. Permo-Carboniferous metamorphosed sedimentary units cover the area. The metamorphosed sediments can be divided into three stratigraphic units which are, from oldest to youngest, Nimri Formation (mainly schist), Keban Marble, and Deli Mehmet Formation (sericite schist including metaconglomerates and limestone lenses). These units are all cut by Tertiary porphyry syenite dykes (Gawlik, 1958; Geoffroy, 1960; Yalçın, 1972; Köksoy, 1978; Özgül, 1981; Yılmaz et al., 1992) (Fig. 3.9).

#### ***3.2.4.2. Mineralization***

Previous studies related with mineralization in the area were carried out by Grannigg (1934), Sündal (1968), Köksoy (1972), Balçık (1979), Çağlayan (1984) and Öztunalı (1985-1989). The mineralization has lense like shape and is located in Permo-Carboniferous Keban Marble on the contact with sericite schists of Deli Mehmet Formation (Köksoy, 1972; Çağlayan, 1984) (Fig.3.10). According to Köksoy (1978), the ore was deposited as both fracture-filling and calcite replacement type before Tertiary. The graphitic layer at the base of the sericite schist (Deli Mehmet Formation) acted as an impermeable barrier to ore-carrying solutions, helping the localization of the ore in the Keban Marble. The dominant ore minerals are galena, sphalarite and pyrite. The mineralization is magmatic-related mesothermal type genetically associated with syenitic intrusions. As a second theory, according to Ziserman (1969), the mineralization in the wall rocks was remobilized by the syenitic intrusion. In addition, Yılmaz et al. (1992) suggested that the Keban mineralization is not directly related with intrusion but can be classified as SEDEX / MVT deposit; the ore minerals were enriched by remobilization with intrusion.

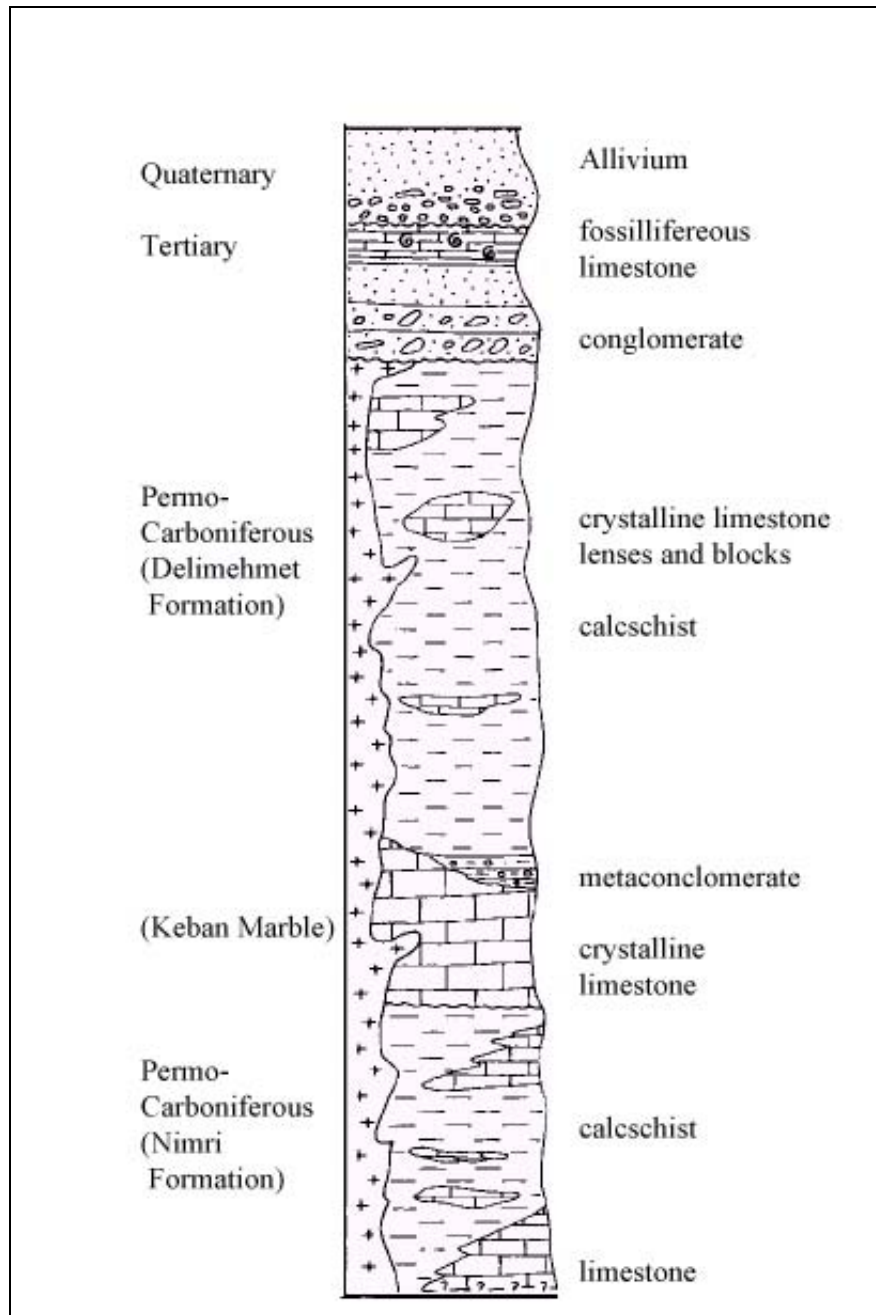


Figure 3.9. Generalized columnar section of Keban area (simplified from Yılmaz et al., 1992)

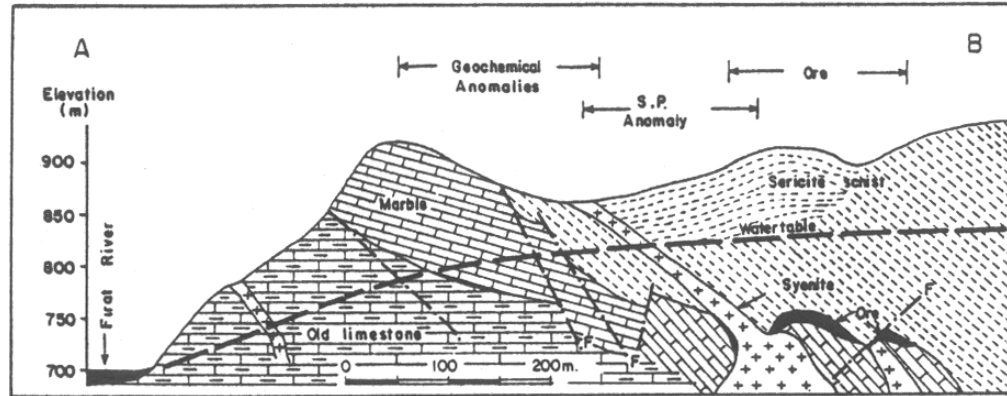


Figure 3.10. Geologic cross-section of the main deposit in Keban area (looking north) (Köksoy, 1978).

### 3.2.5. Bitlis Area (Zizan)

#### 3.2.5.1. Geologic outline

The mineralization is located on the southern part of Bitlis Massif (Eastern Taurides) which consists of a large number of northward dipping slices of metamorphic and sedimentary rocks (Fig. 3.11).

The basement rocks of the massif comprises various gneisses, amphibolites and micaschists (Sengun, 1995). Although an age of about 450 my (based on the Rb-Sr dating) is suggested by Helvacı and Griffin (1984) for the basement, according to Okay (1986), the basement is Precambrian and overlain by a low-grade metamorphic sequence of Early Paleozoic age. The lower limestone part of this sequence is followed by olistostromal felsic metavolcanic/volcanoclastic rocks with blocks of recrystallized limestone and the sequence is intruded by granitoids of Carboniferous age (Göncüoğlu, 1984). Permian-Lower Triassic platformal carbonates unconformably cover these rocks (Göncüoğlu et al., 1996-1997)

The initiation of Alpine cycle is characterized by Middle Triassic metavolcanics and volcanoclastics which are conformably overlain by a condensed series, consisting mainly of metapelites interlayered with basic metavolcanics, metacherts and metatuffs of Late Triassic- Early Cretaceous age. Ophiolites and

ophiolitic olistostromes of Late Cretaceous age are observed as thrust sheets on the metamorphics. Overstep sequences in Bitlis Massif are represented by Middle Eocene shallow marine sediments (Yılmaz, 1975; Yazgan, 1984; Göncüoğlu and Turhan, 1997) (Fig. 3.12).

### 3.2.5.2. Mineralization

Mineralization can be observed in Permian marble and on marble-schist contact. Main minerals are sphalerite, chalcopyrite and pyrite. N-S structures (fractures and faults) host the smithsonite and minor coarse, honey coloured sphalerite and coarse galena.

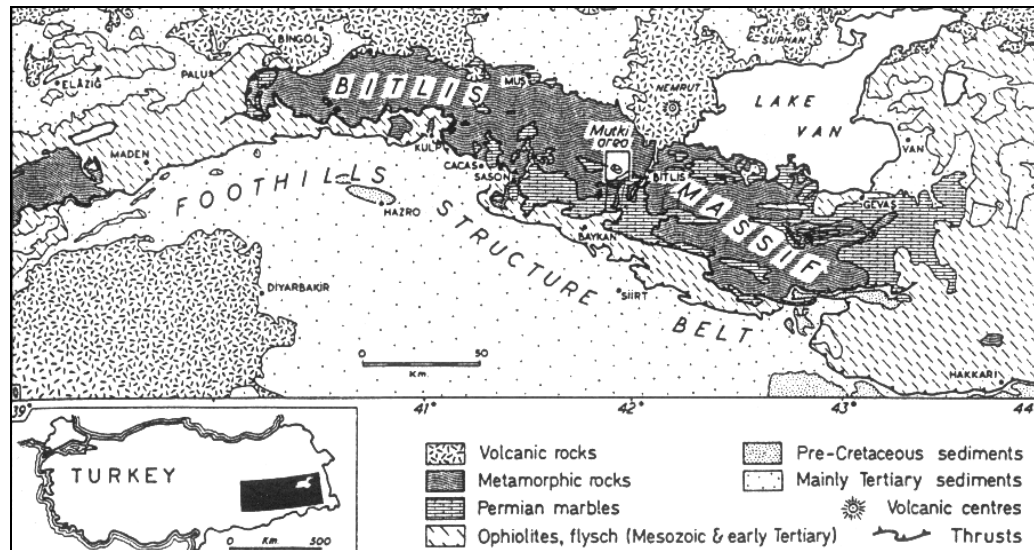


Figure 3.11. Generalized geologic map of southeastern Taurus Mountains (Hall, 1976)

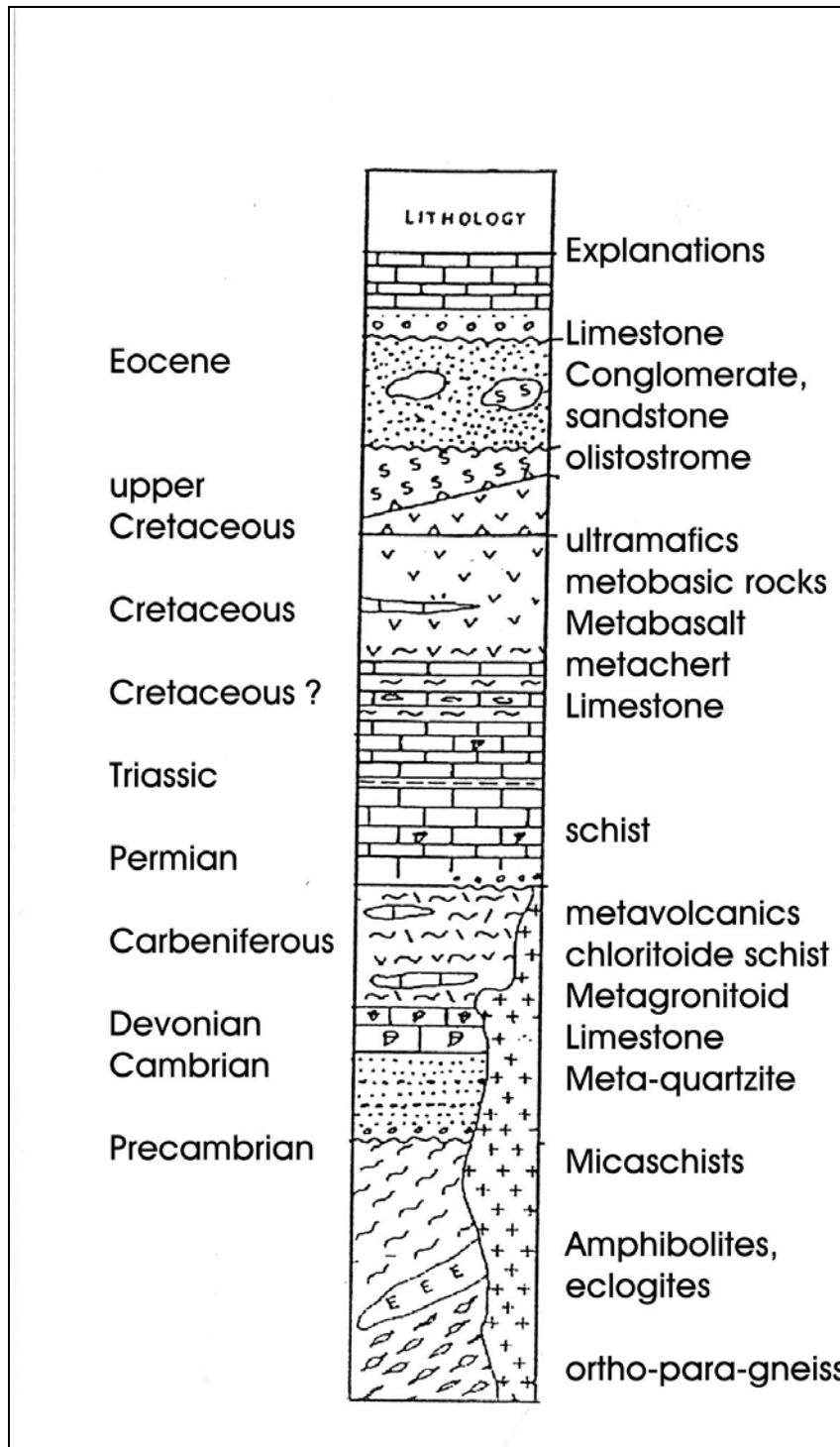


Figure 3.12. Generalized columnar section of the Bitlis Metamorphic Complex (Göncüoğlu and Turhan, 1997).

### **3.3. Studied Areas in Central Anatolian Crystalline Complex (CACC)**

#### **3.3.1. Niğde Area**

##### ***3.3.1.1. Geologic Outline***

The area is located in the Niğde Massif which forms the southeastern corner of the CACC bounded by the Ecemiş Fault in the east. The Niğde Massif, together with the Kırşehir Massif in the north, is commonly interpreted as an integral part of Central Anatolian Crystalline Complex (CACC) (Göncüoğlu et al., 1991) which consists of an assemblage of pre-Cretaceous metamorphic rocks, ophiolitic rocks obducted onto the metamorphics, and the magmatic rocks intruding the both.

In Niğde Massif, the lowest unit is Gümüşler Formation, consisting of gneisses, schists, amphibolites, lenses of marbles. Above this formation, a thick quartzitic band is followed by an alternation of marbles, gneisses, amphibolites and quartzites, namely Kaleboynu Formation. The upper unit of the Niğde Massif consists of a thick sequence of marbles (Aşıgediği Formation) passing upward into cherty marbles and finally into cherts and schists (Göncüoğlu, 1982, 1986; Whitney and Dilek, 1997) (Fig. 3.13). Göncüoğlu et al (1992) suggests a Triassic-Early Cretaceous age for this upper unit of the metamorphic sequence. These metamorphic rock units are overlain by Mesozoic ophiolites with a tectonic contact. The metamorphics as well as the ophiolites are intruded by syn/post collision-type granitoides (Göncüoğlu and Türeli, 1994). The intrusive is named as Üçkapılı Granodiorite in Niğde Area which is Cenomanian (95 my) in age (Göncüoğlu, 1982, 1986; Göncüoğlu et al., 1996-1997). According to Gautier et al. (2002), the granite is older than the Eocene.

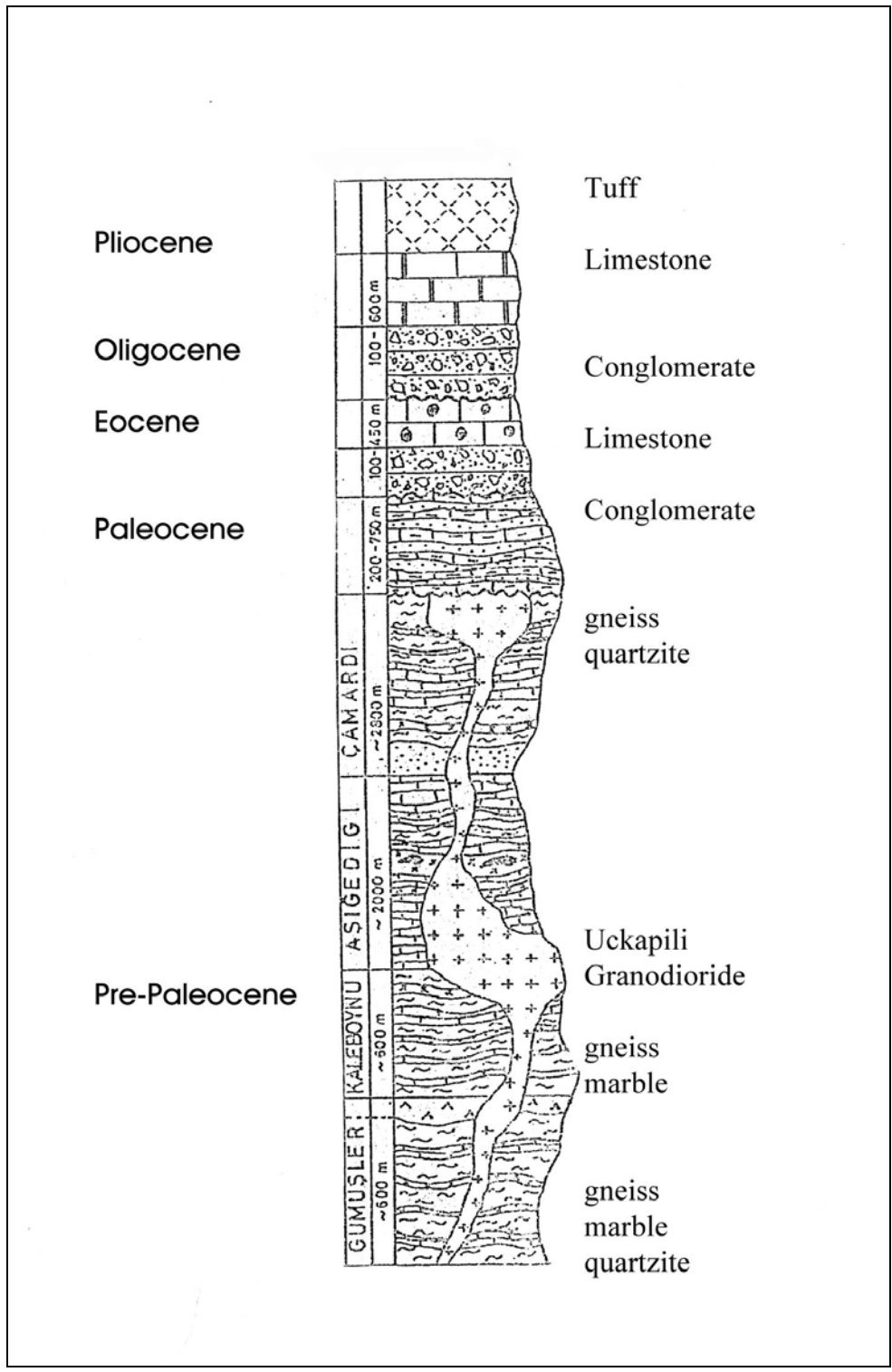


Figure 3.13. Generalized columnar section of Niğde Massif (Pehlivan et al., 1986).

### **3.3.1.2. Mineralization**

As an important metallogenic area, Niğde Massif includes Au, Sn, Ag, Hg, Sb, As, Pb, Zn, Cu, Fe mineralizations which occur within marbles and along marble-schist contacts. Granitic intrusion has an important role for the genesis of ore bodies. Mineralizations are in different types and controlled by structure, lithology and tectonics. According to previous studies (Kovenko, 1944; Imrech, 1964; Özgüneyli, 1978), main mineralization types are contact metasomatic, and vein-type which is controlled by both lithology and structure. The ore minerals are mainly Zn-oxide and sulphide minerals. According to Pehlivan et al. (1986), ore and gang mineral studies suggest multistage mineralization including mesothermal and epithermal stages.

In general, mineralization is related with Üçkapılı granodiorite and located:

- on/near the contact of granodiorite and Niğde metamorphics
- on the gneiss-marble and schist-marble contacts

## **3.4. Studied Areas in Arabian Platform**

### **3.4.1. Hakkari Area**

#### **3.4.1.1. Geologic Outline**

The regional geology of the Hakkari area was studied by Türkünal (1980). Other studies are mostly carried out by TPAO for petroleum exploration purposes (e.g., Altınlı, 1953; Perinçek 1980, 1990).

Perinçek (1990) in his study reports that the oldest unit of the region is represented by the Lower Cambrian clastics. The Middle Cambrian carbonate sequence (Koruk Formation) overlies the clastics and grades into clastics of Late Cambrian to Ordovician age (Habur Group). The Upper Devonian strata directly overlie the Ordovician rocks and consists of interbedded sandstones and limestones (Yığınlı Formation) in the lower part, and shales with limestones (Köprülü

Formation) in the upper part. The Köprülü Formation is covered by the Carboniferous limestones (Belek Formation). The Upper Permian thin sandstones and thick limestones (Tanin Group) transgressively overlie the strata following the regional time break (Fig. 3.14).

No apparent break in sedimentation between the Paleozoic and Mesozoic is observed. The Lower Triassic beds (Çığılı Group) are divided into three formations. The lower and upper formations are composed of interbedded limestones and marls, whereas a reddish terrigenous mudstone occurs in the middle. Carbonate deposition continued during the Middle-Late Triassic to Early Jurassic (Çanaklı Formation), and Late Jurassic-Early Cretaceous (Latdağı Formation) times. Following a regional unconformity, the Mardin Group (Aptian-Turonian) was deposited with basal clastics (Areban Formation), and continued its deposition with shallow marine carbonates (Derdere Formation) which are unconformably overlain by either shales and argillaceous limestones (Ortabağ Formation) or clayey limestones (Sayındere Formation). These formations are Campanian in age, and overlain by either marls and argillaceous limestones (Bozova Formation) or marl-shale-sandstone alternation (Germav Formation, Maastrichtian-Paleocene in age). In the northwestern part of the study area, Maastrichtian sedimentation began with non-marine units (Kıradağ Formation), and continued with marine shale-sandstone alternation. Around the Cilo Mountains, allochthonous units (Koçali Complex), which were emplaced as nappes during the Campanian time, are composed of radiolarite-tuff-agglomerate-basalt-limestone alternation, an ophiolitic slice and Triassic marble blocks. The Koçali Complex and the Germav Formation are covered by the basal clastics of the carbonate sequence (Midyat and Silvan Groups) deposited during the Eocene-Miocene time. There is a break in sedimentation before the Early Miocene. The Lower Miocene limestones (Fırat Formation) are overlain by the non-marine clastics (Şelmo Formation) of Late Miocene age (Perinçek 1990).

Second allochthonous group (Hakkari Complex, Yüksekova Complex and metamorphics) overthrust on to the Şelmo Formation after the Late Miocene time (Fig. 3.14.). The region was affected by compressional forces originated from



different directions during the Late Cretaceous and Late Miocene times (Perinçek 1990).

#### ***3.4.1.2. Mineralization***

Mineralization is hosted by Mesozoic carbonates and main minerals are smithsonite and hydrozincite. Massive ore bodies are seen as stratabound layers and as fracture fillings. Low grade mineralizations are observed as matrix of limestone breccias (Fig. 3.15). No intrusive body is seen in the mineralized area and its vicinity.



Figure 3.15. Zn-Oxide mineralization as matrix of limestone breccias.

## CHAPTER 4

### BASIC PRINCIPLES OF Pb ISOTOPES

#### 4.1. Introduction

Elegant discussions of Pb isotope geochemistry are presented by Doe (1970), Faure (1977), and Dickin (1995). Tosdal et al (1999) summarizes the applications of Pb isotopes to achieve an understanding ore genesis process. The following discussions are from these sources.

The discovery of radioactivity and the subsequent work of the Curies, Rutherford, Soddy, Thomson, Ramsay, and others had a profound effect on geology. In 1903, Cruie and Laborde (in Faure, 1977) demonstrated that radioactive decay is an exothermic process. This started a new line of research by geologists to measure the radioactivity of rocks and to calculate the rate of heat production.

Radioactivity not only causes heat generation in rocks but also provides an accurate method of measuring the ages of rocks and minerals. This possibility was recognized by both Rutherford and B. B. Boltwood around 1905 (Faure, 1977).

#### 4.2. Basic Principles

The composition of atoms is conveniently described by specifying the number of protons and neutrons that are present in the nucleus. The number of protons ( $Z$ ) is called the 'atomic number' and the number of neutrons ( $N$ ) is the 'neutron number'. The atomic number  $Z$  also indicates the number of extranuclear electrons in neutral atom. The sum of protons and neutrons in the nucleus of an atom is the 'mass number', ( $A$ ). We can therefore represent the composition of the nuclei of atoms by means of the simple relationship

$$A = Z + N$$

Another word for atom that is widely used is ‘nuclide’. We can specify the composition of any nuclide by means of a shorthand notation consisting of the chemical symbol of the element, the mass number written as a superscript, and the atomic number written as a subscript. For example,  $^{14}_6\text{C}$  identifies the nuclide as an atom of carbon having 6 protons (therefore 6 electrons in a neutral atom) and an atomic mass of 14. Using the equation, we calculate that the nucleus of this nuclide contains  $14 - 6 = 8$  neutrons. We are now in a position to define several additional terms. Referring to the chart of nuclides (Fig. 4.1), we see that each element having a particular atomic number  $Z$  is represented by several atoms arranged in a horizontal row having different neutron numbers. Such atoms, which have the same  $Z$  but different values of  $N$ , are called ‘isotopes’. Because they have the same  $Z$ , isotopes are atoms of the same chemical element. They have very similar chemical properties and differ only in their masses (Faure, 1977).

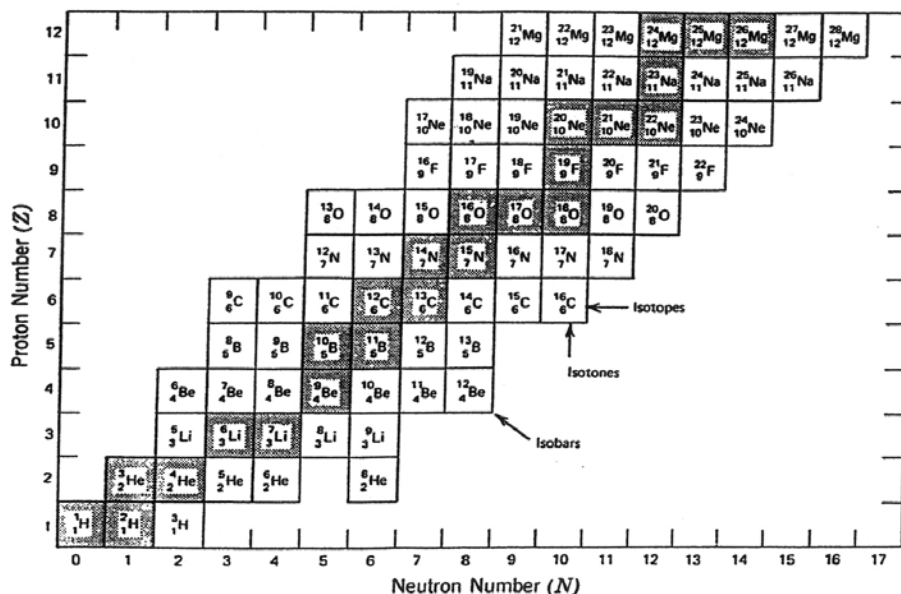


**Figure 4.1.** Partial chart of the nuclides. Each square represents a particular nuclide which is defined in terms of the number of protons ( $Z$ ) and neutrons ( $N$ ) that make up its nucleus. The shaded squares represents stable atoms, while the white squares are the unstable or radioactive nuclides (Faure, 1977).

Isotopes are classified into two groups, namely, radioactive isotopes and stable isotopes. Radioactive isotopes are those that are transformed, through radioactive decay, into other elements. During the decay process the original unstable radioactive isotope is termed the 'parent' and newly formed decay product is the 'daughter' or 'radiogenic'.

Major decay mechanisms are as follows:

Gamma emission occurs when an excited nucleus decays to a more stable state. A gamma ray is simply a high-energy photon (i.e. electromagnetic radiation).

Alpha decay is the emission of alpha particle from a nucleus. An  $\alpha$ -particle is simply a helium nucleus ( ${}^4_2\text{He}$ ). Since the helium nucleus is particularly stable, it is not surprising that such a group of particles might exist within the parent nucleus before  $\alpha$ -decay. Emission of an alpha particle decreases the mass of the nucleus by the mass of the alpha particle.

Beta ( $\beta$ ) decay is transformation of a neutron into a proton and an electron. In this process the atomic number changes but the atomic mass stays constant.

Another type of reaction is electron capture. When an electron is captured, it reacts with proton and produce a neutron (i.e. radioactive parent isotope and radiogenic daughter isotope have different atomic numbers but same atomic mass- the same effect with  $\beta$  decay).

Decay equation for radioactive isotopes is expressed as:

$$N = N_0 e^{-\lambda t} \quad \text{where}$$

$N$ = amount of radioactive (parent) isotope at any time  $t$

$N_0$ = initial amount of radioactive isotope

$\lambda$ = radioactive decay constant

$t$  = time elapsed since the start of radioactive decay

the minus sign indicates that the rate of decay decreases with time.

For radiogenic (daughter) isotope

$$D = D_0 + D^*$$

$$D^* = N_0 - N$$

$$D^* = N(e^{\lambda t} - 1) \quad \text{where}$$

D= amount of daughter isotope present in the system

D<sub>0</sub>= initially present amount of daughter isotope

D\*= amount of radiogenic (daughter) isotope produced by decay of radioactive isotope at any time t

### 4.3. Pb Isotope Geochemistry

Of the four stable isotopes of lead (<sup>204</sup>Pb, <sup>206</sup>Pb, <sup>207</sup>Pb, <sup>208</sup>Pb), only <sup>204</sup>Pb is non-radiogenic. The other lead isotopes are the final decay products of three complex decay chains from uranium (U) and thorium (Th). However, the intermediate members of each series are relatively short-lived, so they can usually be ignored when geological time-scales of millions of years are involved (Dickin, 1995).

Three isotopes, <sup>208</sup>Pb, <sup>207</sup>Pb, and <sup>206</sup>Pb, are partly the radiogenic daughter products from the radioactive decay of one isotope of thorium (<sup>232</sup>Th → <sup>208</sup>Pb\*) and two isotopes of uranium (<sup>238</sup>U → <sup>206</sup>Pb\* and <sup>235</sup>U → <sup>207</sup>Pb\*). (Note that an asterisk (\*) after an isotope denotes that it is the product of radioactive decay of a parent isotope over time and is not the total abundance of the isotope in a sample). The abundance of radiogenic isotopes has grown since the earth formed some 4.56 billion years ago (Fig. 4.2), building upon an initial concentration.

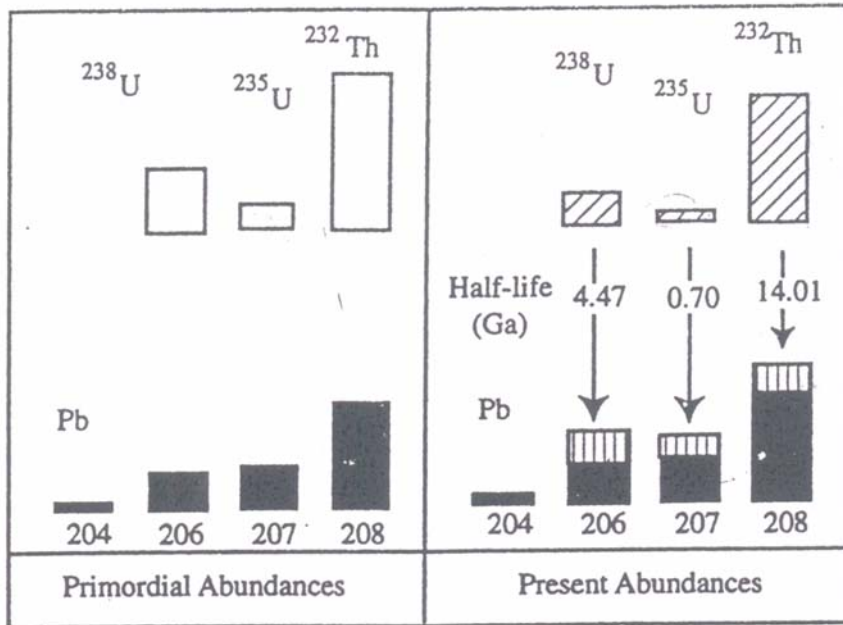


**Figure 4.2.** Relative primordial and present-day abundance of the isotopes of uranium (U), thorium (Th), and lead (Pb) showing half-lives in billion of years (Ga). Modified from Cannon et al (1961) and Gulson (1986)

The fourth isotope of Pb,  $^{204}\text{Pb}$ , is stable and has no long-lived parent isotope nor does it decay to another isotope. Time-integrated growth of radiogenic Pb isotopes from an arbitrary starting time,  $t_0$ , to an ending time,  $t_1$ , in an environment where there has been no migration of U, Th, and their daughter products, is described by standard decay equations:

$$(^{206}\text{Pb}/^{204}\text{Pb})_{t_1} = (^{206}\text{Pb}/^{204}\text{Pb})_{t_0} + (^{238}\text{U}/^{204}\text{Pb})(e^{\lambda t_0} - e^{\lambda t_1})$$

$$(^{207}\text{Pb}/^{204}\text{Pb})_{t_1} = (^{207}\text{Pb}/^{204}\text{Pb})_{t_0} + (^{235}\text{U}/^{204}\text{Pb})(e^{\lambda' t_0} - e^{\lambda' t_1})$$

$$(^{208}\text{Pb}/^{204}\text{Pb})_{t_1} = (^{208}\text{Pb}/^{204}\text{Pb})_{t_0} + (^{232}\text{Th}/^{204}\text{Pb})(e^{\lambda'' t_0} - e^{\lambda'' t_1})$$

where  $\lambda$ ,  $\lambda'$ , and  $\lambda''$  are the decay constants of  $^{238}\text{U}$ ,  $^{235}\text{U}$ , and  $^{232}\text{Th}$ , respectively (see Table 4.1 for explanation of constants and symbols). These equations simply show that the measured present-day Pb isotope composition is equal to the sum of

the initial Pb isotope composition plus radiogenic Pb added over time. Because  $^{204}\text{Pb}$  is stable and therefore fixed, and because the abundances of  $^{208}\text{Pb}$ ,  $^{207}\text{Pb}$ , and  $^{206}\text{Pb}$  change over time and are difficult to measure directly, Pb isotope data are examined as the ratio of a radiogenic isotope to the stable isotope, or  $^{208}\text{Pb}/^{204}\text{Pb}$ ,  $^{207}\text{Pb}/^{204}\text{Pb}$ , and  $^{206}\text{Pb}/^{204}\text{Pb}$  (Tosdal et al., 1999).

**Table 4.1.** Constants and symbols critical to Pb isotope geochemistry (Tosdal et al., 1999)

Symbol	Value	Explanation
$\lambda_1$	$0.155125 \times 10^{-9}/\text{a}$	Decay constant of $^{238}\text{U}$
$t^{1/2}$	4.47 Ga	Half-life of $^{238}\text{U}$
$\lambda_2$	$0.98485 \times 10^{-9}/\text{a}$	Decay constant of $^{235}\text{U}$
$t^{1/2}$	0.70 Ga	Half-life of $^{235}\text{U}$
$\lambda_3$	$0.49475 \times 10^{-10}/\text{a}$	Decay constant of $^{232}\text{Th}$
$t^{1/2}$	14.01 Ga	Half-life of $^{232}\text{Th}$
$\mu$	Variable	$^{238}\text{U}/^{204}\text{Pb}$
$\kappa$	Variable	$^{232}\text{Th}/^{238}\text{U}$

‘Common lead’ is any lead from a phase with low value of U/Pb and/or Th/Pb that no significant radiogenic lead has been generated *in situ* since the phase formed. Such phases are galena and other sulfides such as pyrite, feldspars and micas. Data on common lead are used in determining ages and, more important, in the solution of genetic problems (Doe, 1970).

In the U-Th-Pb system, the presence of two long-lived isotopes of U decaying to two separate isotopes of Pb is a unique and powerful feature. The coupling of the decay of  $^{238}\text{U}$  to  $^{206}\text{Pb}^*$  and  $^{235}\text{U}$  to  $^{207}\text{Pb}^*$  provides a time control on Pb isotope compositions at different times during the earth’s history. For example, because the half-life of  $^{235}\text{U}$  is so much shorter than that of  $^{238}\text{U}$  (Table 4.1), there was a rapid increase in  $^{207}\text{Pb}$  with respect to  $^{206}\text{Pb}$  during the earth’s early history (Fig. 4.3). The rate of  $^{207}\text{Pb}$  growth diminishes with time as the parent  $^{235}\text{U}$  disappears due to radioactive decay. In essence,  $^{207}\text{Pb}$  growth over the last billion years has been negligible (Doe, 1970; Tosdal et al., 1999).

In order to understand Pb isotope variations, two other parameters, the U/Pb and Th/U ratios (Table 4.2), are important, as is a basic understanding of U, Th, and Pb

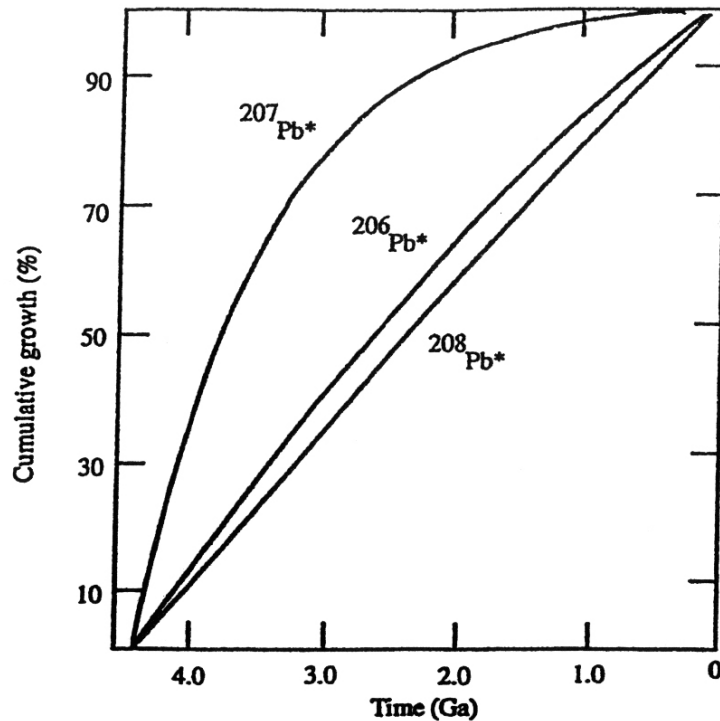


**Figure 4.3.** Time (Ga) vs Cumulative growth (%) of radiogenic Pb. Growth of radiogenic Pb with time showing the rapid increase in  $^{207}\text{Pb}^*$  in the early history of the earth because of the relatively short half-life of  $^{235}\text{U}$  (700 m.y.) followed by only limited growth in  $^{207}\text{Pb}^*$  in the last 1.0 billion years (Ga). The limited growth of  $^{207}\text{Pb}^*$  results from the fact that most  $^{235}\text{U}$  has already decayed, and only a small fraction of the original primordial abundance is still present. Modified from Garipey and Dupre (1991)

geochemical properties (Faure, 1977). U and Th are usually in tetravalent oxidation states and have comparable geochemical properties in nature. They, thus, commonly act together and substitute for each other in compounds. For example, during partial melting and fractional crystallization, U and Th are concentrated in the liquid phase in favor of the residual from melting or the crystallized parts of the magma. In contact with aqueous fluids, however, Th is

insoluble and is one of the inert elements (Taylor and McLennan, 1985). U, in contrast to Th, has a second oxidation state. Under oxidizing conditions, U forms uranyl ions (+6) that are extremely soluble in aqueous fluids. Under these conditions, U may be significantly fractionated from Th. Lead is soluble at the moderate to high temperatures found in hydrothermal, magmatic, or metamorphic environments, whereas at low temperature it is easily complexed with organic matter but generally is not soluble. Lead is also a larger ion than the parent elements U or Th, and thus, will exhibit different behavior during events such as partial melting, metamorphism, or low-temperature alteration. The contrasting geochemical behavior of U, Th, and Pb in different geological environments is recorded in the Th/U ( $\kappa$  or  $^{232}\text{Th}/^{238}\text{U}$ ) and U/Pb ( $\mu$  or  $^{238}\text{U}/^{204}\text{Pb}$ ), which can be directly measured as elemental concentrations, calculated using model parameters, or inferred from Pb isotope data (Tosdal et al., 1999).

**Table 4.2.** Present-day U-Th-Pb compositions of the Crust-Mantle system (adapted from Allegre et al., 1988; Gariépy and Dupre, 1991)

	Bulk earth	Depleted mantle	Continental crust
U (ppb)	21	3.5	1,200
Th (ppb)	88	8.5	5,800
Pb (ppb)	170	50	8,600
$^{238}\text{U}/^{204}\text{Pb}$	9.1	4.7-5.9	10.6-10.8
$^{232}\text{Th}/^{238}\text{U}$	4.2	2.3-2.5	4.6-4.7

Lead isotope data are typically presented on two covariation diagrams (Fig. 4.4). One diagram, also referred to as the thorogenic diagram, plots  $^{208}\text{Pb}/^{204}\text{Pb}$  versus  $^{206}\text{Pb}/^{204}\text{Pb}$  or the radiogenic daughter of Th versus the radiogenic daughter of the most abundant U isotope (Fig. 4.4A). The other diagram, also referred to as the uranium diagram, plots  $^{207}\text{Pb}/^{204}\text{Pb}$  versus  $^{206}\text{Pb}/^{204}\text{Pb}$ , or the least abundant isotope of U versus the most abundant (Fig. 4.4B). There are three idealized crustal reservoirs of U-Th-Pb: the mantle, lower crust and upper crust. These reservoirs mix in the orogene where crustal deformation, magmatism, sedimentation, and metamorphism take place (Zartman and Doe, 1981).

Discussion of Pb isotope data on covariation diagrams is made with reference to a model Pb isotope growth curve derived from worldwide Pb isotope values. The most widely used curves are the average crustal growth curves of Stacey and Kramers (1975) and Cumming and Richards (1975). These curves are model representations of the Pb isotope evolution of continental crust based upon Pb isotope compositions of galena from ore deposits whose hydrothermal systems averaged large segments of crust. The average crustal growth curve of Stacey and Kramers (1975) is based on two stages of growth characterized by different U/Pb and Th/U. In contrast, the average crustal growth curve of Cumming and Richards (1975) is based on the continuous evolution of U/Pb and Th/U through time. The use of one or the other growth curve in Pb isotope studies is a matter of preference. These growth curves are important because they provide reference crustal value to compare Pb isotope compositions measured in rocks and minerals.

From a practical standpoint, the average crustal growth curve of Stacey and Kramers (1975) approximates the orogene curve of Zartman and Doe (1981), whereas the average crustal curve of Cumming and Richards (1975) resembles the upper crustal growth curve of Zartman and Doe (1981) (Fig 4.4).

Average crustal growth curves are used for the presentation of Pb isotope compositions of ore minerals, their sources and rocks. According to Doe and Zartman (1979), rocks in the lower crust have greater Th/U values than average crust (Fig 4.4). Therefore measured  $^{208}\text{Pb}/^{204}\text{Pb}$  of lower crustal rocks at a given  $^{206}\text{Pb}/^{204}\text{Pb}$  value lie above the average crustal growth curve of Stacey and Kramers (Th/U = 3.8) (1975). Whereas island arcs, ocean island basalts and chemical sediments (e.g., limestone) have Th/U values less than that of average crust (Doe, 1970; Tatsumoto, 1978; Taylor and McLennan, 1985). Average continental crust has a U/Pb value of 9.74 (Stacey and Kramers, 1975). Measured Pb isotope compositions having lower  $^{207}\text{Pb}/^{204}\text{Pb}$  indicate that this Pb evolved in environment with U/Pb values lower than that of average crust or vice versa. In addition, Doe and Zartman (1979) point out that elevated  $^{207}\text{Pb}/^{204}\text{Pb}$  values are indicative of regions of the crust where radiogenic Pb evolved in Archean rocks because of limited production of  $^{207}\text{Pb}$  over the last billion years. Conversely,

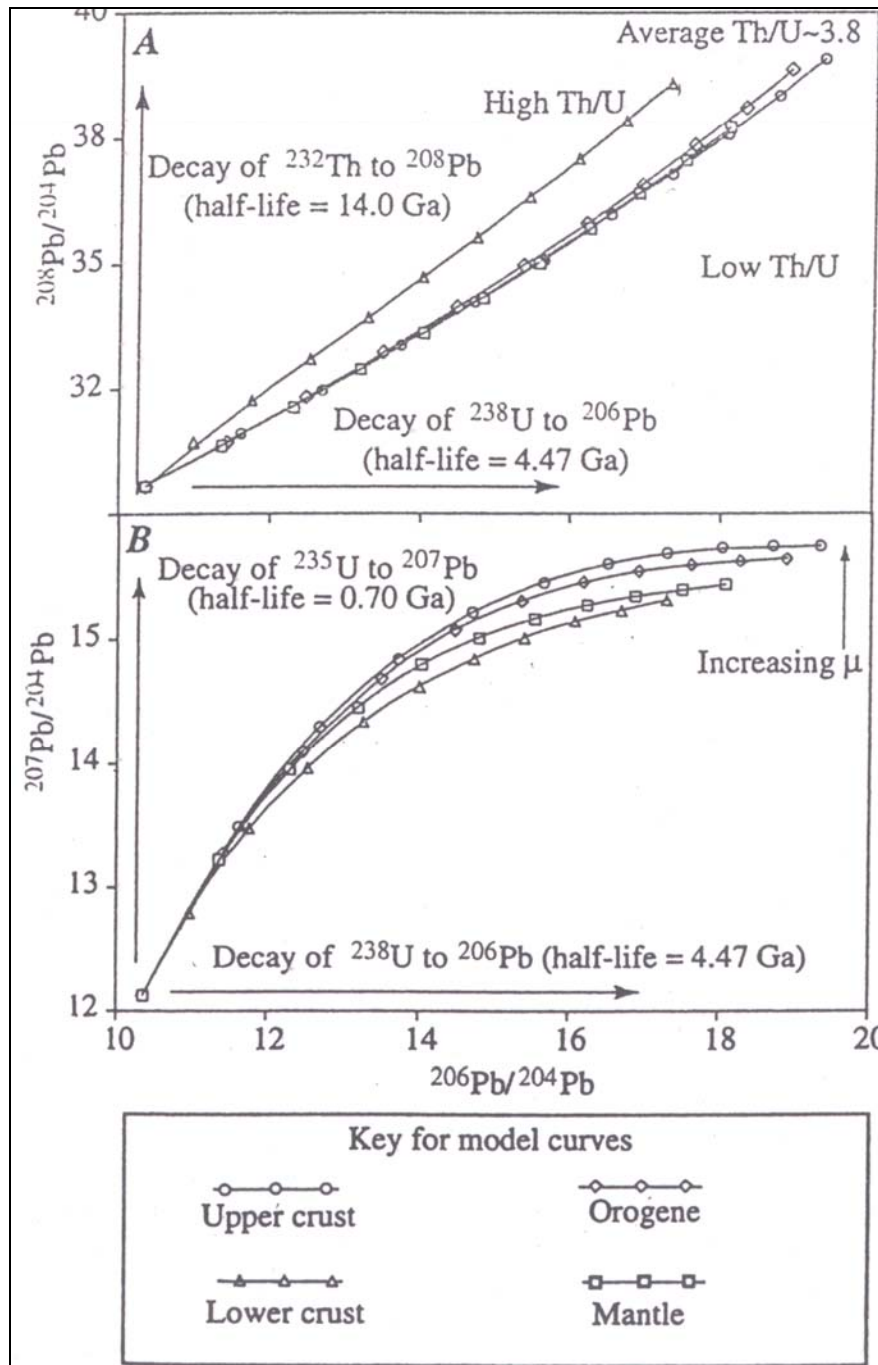


**Figure 4.4.** Thorogenic (A) and Uranogenic (B) Pb isotope diagrams showing the plumbotectonic curves of Zartman and Doe (1981). Tick marks on curves represent 500 million years of growth.

lower  $^{207}\text{Pb}/^{204}\text{Pb}$  values indicate a lack of old radiogenic Pb. Therefore changes on uraniumogenic diagram are a function of time or age of formation, as recorded by the changing  $^{206}\text{Pb}/^{204}\text{Pb}$  values, and the relative input of primitive versus old crustal Pb as recorded by the  $^{207}\text{Pb}/^{204}\text{Pb}$  values.

Tosdal et al (1999) stated that when applying Pb isotope compositions of rocks and ore minerals to understanding sources of magma, metals and fluid-rock interactions, it is important to bear in mind that there are usually differences in Pb concentration between sources encountered during magma ascent or fluid flow and subsequent crystallization and deposition. If a low Pb concentration characterizes a magma or hydrothermal fluid, then interactions with country rocks can change Pb isotope compositions of the magma and fluid. Pb isotope compositions of samples in these situations will reflect mixed sources. This is illustrated by the interaction of mantle-derived magmas and continental crust. Magmas derived from the mantle have intrinsically low Pb concentrations (1-2 ppm or less) relative to feldspar-rich crustal rocks that principally have 10 to 30 ppm Pb. Because of the strong contrast in Pb concentration, incorporation of a little crustal Pb can significantly modify the Pb isotope composition of a mantle-derived basaltic magma. Hence, the Pb isotope composition of most granitic rocks reflects that of the crust with which it is associated even if the magma had a significant mantle contribution to its formation (Davidson, 1996). A similar line of reasoning would also apply to hydrothermal fluids. On the other hand, if the magma or hydrothermal fluid contains normal crustal concentrations of Pb, then it is more difficult to change the Pb isotope composition significantly through magma assimilation or fluid-rock interaction. Pb isotope evidence for such interactions is either limited or lacking. However, the absence of Pb isotope evidence by no means precludes the event from having occurred.

#### **4.4. Pb Isotopes in Ore Deposits**

Pb is common in ore deposits, either in the primary Pb sulfide galena or as a major or trace element in other sulfide or sulfosalt minerals. These Pb isotope compositions are easily measured. Because the concentration of U with respect to

Pb in ore minerals is intrinsically low, time integrated growth in the Pb isotope composition is minimal to negligible for minerals formed in Phanerozoic. For this reason, if the system remained closed, measured Pb isotope composition approximates the composition of the mineral and hydrothermal fluid at the time of crystallization. In contrast, for ore minerals of Proterozoic and Archean ages, there has been sufficient time for some radiogenic growth of Pb because U is not completely excluded from some common sulfide minerals such as pyrite and chalcopyrite. Measured Pb isotope compositions of these old minerals need to be corrected for time-integrated growth to obtain an initial composition (Tosdal et al., 1999).

As indicated by Arribas and Tosdal (1994) and Tosdal et al (1999), because of the Precambrian Pb isotope heterogeneity, local Pb isotope growth curves applicable to specific crustal region need to be constructed before the Pb isotope data can have any absolute chronologic significance.

The use of Pb isotopes to determine source(s) of Pb in ore deposits involves direct measurement of Pb isotope compositions of a Pb-bearing mineral. Their utility for determining the source of associated metals Zn, Cu, Au, Ag and other metals is limited by the assumption that Pb was derived from the same source, transported, and deposited from the same hydrothermal fluid. This assumption is for the most part true because of the comparable geochemical behavior of Pb, Zn and Cu in hydrothermal fluids (Henley et al., 1984), particularly in base metal-rich magmatic hydrothermal systems or Pb-rich deposits in sedimentary environments. Combining Pb isotope data with Re-Os data on sulfides and Rb-Sr and Sm-Nd data on gangue and ore minerals can provide important constrains on metal sources and fluid-rock interactions.

For evaluating Pb sources and by inference sources of associated metals in any hydrothermal system, it is not sufficient to know just the Pb isotope composition of the ore minerals. To utilize the power of Pb isotopes fully, it is also critical to know the Pb isotope compositions of rock reservoirs through which a particular hydrothermal fluid may have flowed.

#### **4.5. Homogeneous versus Heterogeneous Pb Sources**

Pb isotope compositions determined in ore deposits vary either from essentially identical or homogeneous ones at various scales within a deposit, district, or metallogenic provinces to a narrow or a broad range of values indicating Pb isotope heterogeneity. Relatively homogeneous Pb isotope compositions of ore minerals result from one of two scenarios (Tosdal et al., 1999):

- The hydrothermal system was sufficiently large that any Pb isotope heterogeneity in the source(s) was averaged as the fluids reacted with rocks along an aquifer,
- Hydrothermal fluids may have emanated from a source, such as a plutonic complex, that did not assimilate or encounter rocks of a different Pb isotope composition at or near the site of emplacement. Such fluids are common in porphyry environment.

At the giant Porgera Au deposit in Papua New Guinea, Richards et al. (1991) documented a narrow Pb isotope range of ore minerals (Fig 4.5). This deposit, consisting of an early 'porphyry-type' stage followed by a superimposed low-sulphidation epithermal stage, is associated with alkaline stocks emplaced into Mesozoic and Cenozoic sedimentary rocks (Richards, 1995). The Pb isotope compositions of the ore minerals are displaced toward the average Pb isotope composition of the sedimentary rock sequences.

On the other extreme, heterogeneous Pb isotope compositions are expected in sedimentary rock-hosted deposits where fluids may have traveled along different aquifers, equilibrated with rocks of different chemical and isotopic compositions, and mixed at the site of ore deposition. Most Mississippi Valley-type (MVT) Pb-Zn deposits in particular show extreme ranges of Pb isotope composition and mixing between multiple reservoirs near the site of ore deposition (Kesler et al., 1994).

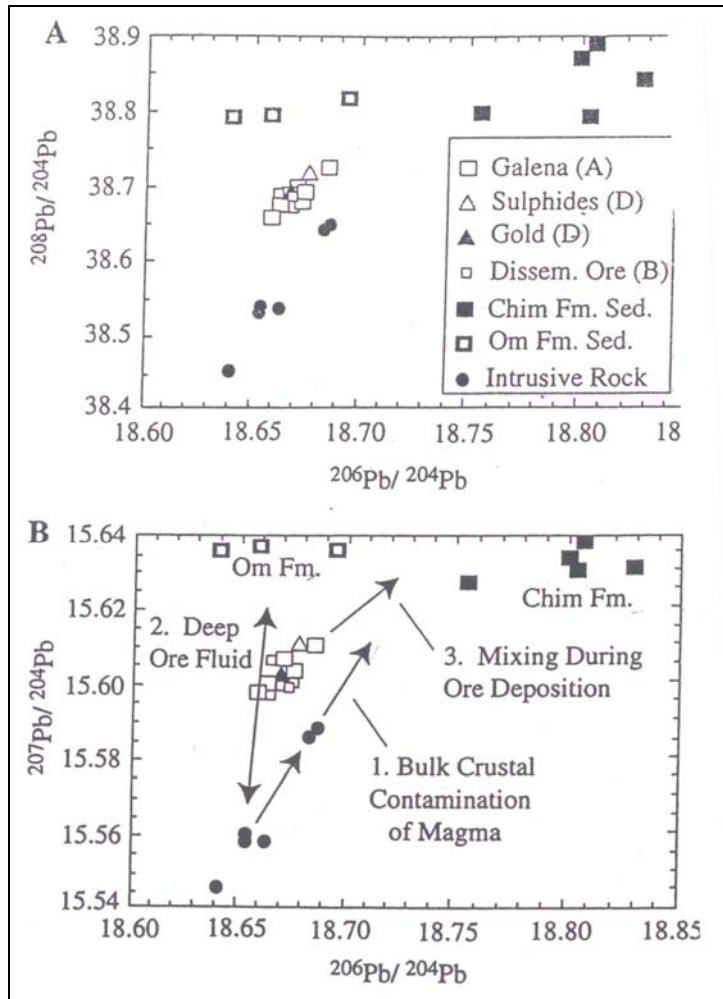


**Figure 4.5.** Mixing of multiple Pb sources at the Porgera Au deposit, Papua New Guinea. Modified from Richards et al. (1991). Thorogenic (A) and uranogenic (B) Pb diagrams show the effect of mixing in the magmatic system (B, Trend 1) and in the hydrothermal system (B, trends 2 and 3).

Pb isotope homogeneity or heterogeneity of ore minerals in a deposit or a district reflects a variety of factors:

- Of importance is the starting isotopic composition of the hydrothermal fluid; in addition is the degree of fluid-rock interactions along fluid pathways .
- Also critical is where the disparate hydrothermal fluids mixed. If mixing was close to the site of ore deposition, then a a range of Pb isotope compositions might be expected.

## CHAPTER 5

### Pb-ISOTOPE COMPOSITIONS OF THE STUDIED MINERALIZATIONS

#### 5.1. Introduction

In this study, a total of 43 galena samples collected from several Pb-Zn occurrences in 7 different areas were examined for their Pb-isotope compositions. The localities of the samples are shown in Appendix A.

Of the 43 samples, 25 are from Zamantı, 6 from K. Maraş, 3 from Malatya, 1 from Elazığ-Keban, 2 from Bitlis-Zizan, and 4 samples are from Hakkari area. The distribution of the samples with respect to the studied areas is shown in Table 5.1.

#### 5.2. Methods of Study

The galena bearing rock samples were taken for Pb isotope analysis from the mineralizations in the studied areas by Teck Cominco Madencilik San. A.Ş. geologists between 2000-2002 years. As a field geologist in the same company, I have worked in most of the studied areas like Zamantı, Keban and Hakkari and made prospecting and geological mapping. The samples were analyzed in Canada in different laboratories (e.g. Geospec Consultants Limited, Canada). Although the standard procedures are used in all the laboratories, precision and accuracy of the results have not checked by using duplicate and standard samples. The analytical technique applied by Geospec Consultants Limited laboratory is as follows:

- The rock samples were cleaned, crushed to a fine chip size and washed.
- Galena concentrates were prepared by hand picking fine galena grains under binocular microscope.
- Good quality galena grains were recovered

- Clean galena grains were carefully selected and dissolved in 2N HCl and gently evaporated to dryness.
- PbCl<sub>2</sub> crystals formed by fractional crystallization were purified in 4N HCl and finally cleaned in super pure H<sub>2</sub>O
- Approximately 500 ng of extracted lead (in PbCl<sub>2</sub> form) is loaded on Rhenium filament using the standard silica gel-phosphoric acid technique and the isotopic composition was measured in a Micromass MM30 mass spectrometer
- Overall reproducibility of the Pb measurement in the laboratory is determined from large number of NBS SRM 981 and SRM 982 Pb standard measurements performed routinely on the instrument.
- Reproducibility of the measured isotopic ratios are at 1 sigma error level
- All of the reported results have been normalized to the nominal NBS SRM 981 Common lead standard values.

### 5.3. Results

The results of Pb-isotope analysis of galena samples are given in Table 5.1, and presented on conventional Pb-isotope co-variation diagrams in Fig 5.1 & 5.2.

As can be seen from Table 5.1, <sup>206</sup>Pb/<sup>204</sup>Pb, <sup>207</sup>Pb/<sup>204</sup>Pb and <sup>208</sup>Pb/<sup>204</sup>Pb ratios of the samples cover a wide range between 18.034 – 19.228, 15.623 – 15.742 and 37.944 – 39.308, respectively. There appears to be no characteristic range pertinent to individual areas; considerable variations exist even in a single area as it is the case with Zamantı and K. Maraş samples (Fig. 5.1 & 5.2). The compositional ranges yielded by Hakkari and Niğde areas are relatively low compared to the other areas, but this is believed to stand from the restricted number of samples collected from these areas (Table 5.1). Further evaluation of the Pb-isotope compositions is given in the next *Discussion* chapter.

Table 5.1. Pb isotope results with relevant informations with UTM coordinates of samples (Lmst: limestone, CRD: Carbonate replacement deposits, MVT: Mississippi Valley type).

Number	UTM Zone (S)	Easting	Northing	Location	$^{206}\text{Pb} / ^{204}\text{Pb}$	$^{207}\text{Pb} / ^{204}\text{Pb}$	$^{208}\text{Pb} / ^{204}\text{Pb}$	Host Rock	Age of host rock	Mineralization in Field Observation
1	36	669033	4189283	Niğde - Celaller	18.771	15.695	38.975	Schist - Marble	pre-Cretaceous	Skarn + CRD
2	36	672600	4194250	Niğde	18.755	15.687	38.928	Marble	pre-Cretaceous	Skarn + CRD
3	36	695948	4224023	Kayseri-(S of <i>Çadırkaya Fe deposit</i> )	18.993	15.688	38.969	Lmst and andesite	Permian	Skarn
4	36	695667	4223847	Kayseri-(S of <i>Çadırkaya Fe deposit</i> )	18,993	15,682	38,955	Lmst and andesite	Permian	Skarn
5	36	689763	4224860	Kayseri (2 km SW of Ismail Inkaya Fe deposit)	19.002	15.682	38.906	Lmst	Permian	Skarn
6	36	730974	4228934	Kayseri ( near Yoncaliseki Zn-Pb-Fe showing)	18.637	15.697	38.784	Lmst	Late Cretaceous	CRD
7	36	707745	4230174	Kayseri-Kocahacılı	18.798	15.717	38.992	Lmst	Permo-Carboniferous	Stockwork

Table 5.1. Pb isotope results with relevant informations with UTM coordinates of samples  
(Lmst: limestone, CRD: Carbonate replacement deposits, MVT: Mississippi Valley type) (continued).

8	36	721400	4226000	Kayseri- ( <i>Denizovası</i> <i>deposit</i> )	18.684	15.704	38.843	Lmst	Carboniferous- Late Permian	Karstic filling along fault zone
9	36	718850	4225080	Kayseri-(W of <i>Denizovası</i> )	18.827	15.720	38.962	Lmst	Devonian	CRD
10	36	701007	4201099	Kayseri-(Near <i>Aladağ- Delikkaya Pb-Zn deposit</i> )	18.6957	15.7193	38.891	Lmst	Late Devonian- Jurassic	CRD
11	36	701300	4201600	Kayseri-(Near <i>Aladağ- Delikkaya Pb-Zn deposit</i> )	18.7096	15.7035	38.8717	Lmst	Late Devonian- Jurassic	CRD
12	36	698130	4200127	Kayseri-( <i>Aladağ- Delikkaya Pb-Zn deposit</i> )	18.8264	15.712	38.9554	Lmst	Late Devonian- Jurassic	Stockwork vein
13	36	699315	4200823	Kayseri-( <i>Aladağ- Delikkaya Pb-Zn deposit</i> )	18.693	15.709	38.891	Lmst	Late Devonian- Jurassic	Stockwork vein
14	36	719448	4225884	Kayseri-( <i>Ayoluğu Zn-Pb deposit</i> )	18.704	15.716	38.892	Lmst	Jurassic- Late Cretaceous	Karstic filling along fault zone

Sample No.	Zone	Easting	Northing	Deposit Type	X <sub>Pb</sub>	Y <sub>Pb</sub>	Z <sub>Pb</sub>	Host Rock	Age	Notes
15	36	694524	4216441	Kayseri- ( <i>Dünderlı Pb-Zn deposit</i> )	19.037	15.73	39.134	Lmst	Devonian-Cretaceous	Fracture and karstic filling
16	36	706923	4206272	Kayseri- ( <i>Suçatı Pb-Zn deposit</i> )	18.758	15.721	38.929	Lmst	Jurassic	Fracture and karstic filling
17	36	755831	4227895	Kayseri- ( <i>Saraycık Pb-Zn deposit</i> )	18.764	15.716	38.928	Lmst	Devonian	Fracture filling conformable with bedding
18	36	726008	4226173	Kayseri- ( <i>Çakılıpınar Zn-Pb deposit</i> )	18.676	15.708	38.868	Lmst-dolomite	Jurassic-Late Cretaceous	Vein
19	36	699841	4219076	Kayseri- ( <i>Dereköy-Ayraklı Zn-Pb deposit 'Oreks'</i> )	18.789	15.72	38.974	Lmst-schist contact and lmst	Devonian	Fracture filling
20	36	699841	4219076	Kayseri- ( <i>Dereköy-Ayraklı Zn-Pb deposit 'Oreks'</i> )	18,896	15,736	39,027	Lmst-schist contact and lmst	Devonian	Fracture filling
21	36	722001	4226727	Kayseri- ( <i>Celaldağı Zn-Pb deposit</i> )	18.682	15.707	38.859	lmst	Late Permian	Along fault zone

Table 5.1. Pb isotope results with relevant informations with UTM coordinates of samples  
(Lmst: limestone, CRD: Carbonate replacement deposits, MVT: Mississippi Valley type) (continued).

22	36	716268	4213132	Kayseri-Ayvan (Sultankuyu Fe Showing)	18.623	15.706	38.832	Lmst	Carboniferous	Karstic filling
23	36	738879	4219785	Kayseri-(Kaleköy Zn-Pb deposit)	18.323	15.688	38.453	Dolomite	Devonian	Vein
24	36	712400	4226000	Kayseri-(Ağcaşar Zn-Pb-Fe deposit)	18,955	15,730	39,022	Lmst	Triassic	Strata bound
25	37	268666	4231456	Adana- Tufanbeyli- Bozcal	18.704	15.713	39.027	Dolomite	Devonian	MVT
26	37	265644	4220990	Adana- Tufanbeyli-Akçal	18,635	15,698	38,916	Dolomite	Devonian	MVT
27	37	264273	4242040	Adana- Tufanbeyli	18.728	15.718	39.064	Dolomite	Devonian	Vein
28	37	318652	4226580	K.Maraş-Afşin	18.869	15.696	39.057	Andesite	Late Cretaceous	Vein
29	37	317883	4232345	K.Maraş-Afşin	19.127	15.73	39.246	Granite	Tertiary	Disseminated
30	37	314240	4231930	K.Maraş-Afşin	19.133	15.742	39.308	Ophiolite		As galena pods
31	37	301200	4234170	K.Maraş-Afşin- Türksevin	18.084	15.658	38.216	Lmst	Permo- Carboniferous	Vein
32	37	329285	4184286	K.Maraş- Engizek-Çiğdem	19.021	15.709	39.221	Lmst	Miocene	Vein

Sample No.	UTM Easting	UTM Northing	Location	X <sub>1</sub>	X <sub>2</sub>	X <sub>3</sub>	Host Rock	Age	Notes	
33	37	328622	4184328	K.Maraş-Engizek-Çal	18.982	15.707	39.125	Lmst	Miocene	Veins along fractures
34	37	403181	4228245	Malatya-Adatepe	19.228	15.623	39.191	Lmst	Permo-Carboniferous	CRD
35	37	425000	4237000	Malatya-Cafana	18.097	15.66	38.279	Lmst	Permo-Carboniferous	CRD
36	37	419600	4218600	Malatya-Cafana-Melet deresi	18,086	15,651	38,240	Marble	Paleozoic	CRD
37	37	475978	4297112	Elazığ- Keban	19.203	15.707	39.227	Marble, Lmst, dolomite	Devonian	Skarn + vein
38	37	759181	4239310	Bitlis-Zizan-Dava	18.718	15.725	37.944	Lmst , Marble	Permian	Vein
39	37	759166	4239454	Bitlis- Lower Zizan	18.731	15.724	38.956	Lmst	Permian	Vein
40	38	SW of	Hakkari	Hakkari	18.412	15.678	38.633	Lmst	Jurassic-Cretaceous	Stratabound
41	38	SW of	Hakkari	Hakkari	18.44	15.68	38.671	Lmst	Jurassic-Cretaceous	Stratabound
42	38	SW of	Hakkari	Hakkari	18.404	15.668	38.633	Lmst	Jurassic-Cretaceous	Stratabound
43	38	SW of	Hakkari	Hakkari	18.408	15.676	38.713	Lmst	Jurassic-Cretaceous	Stratabound

### Uranogenic Diagram

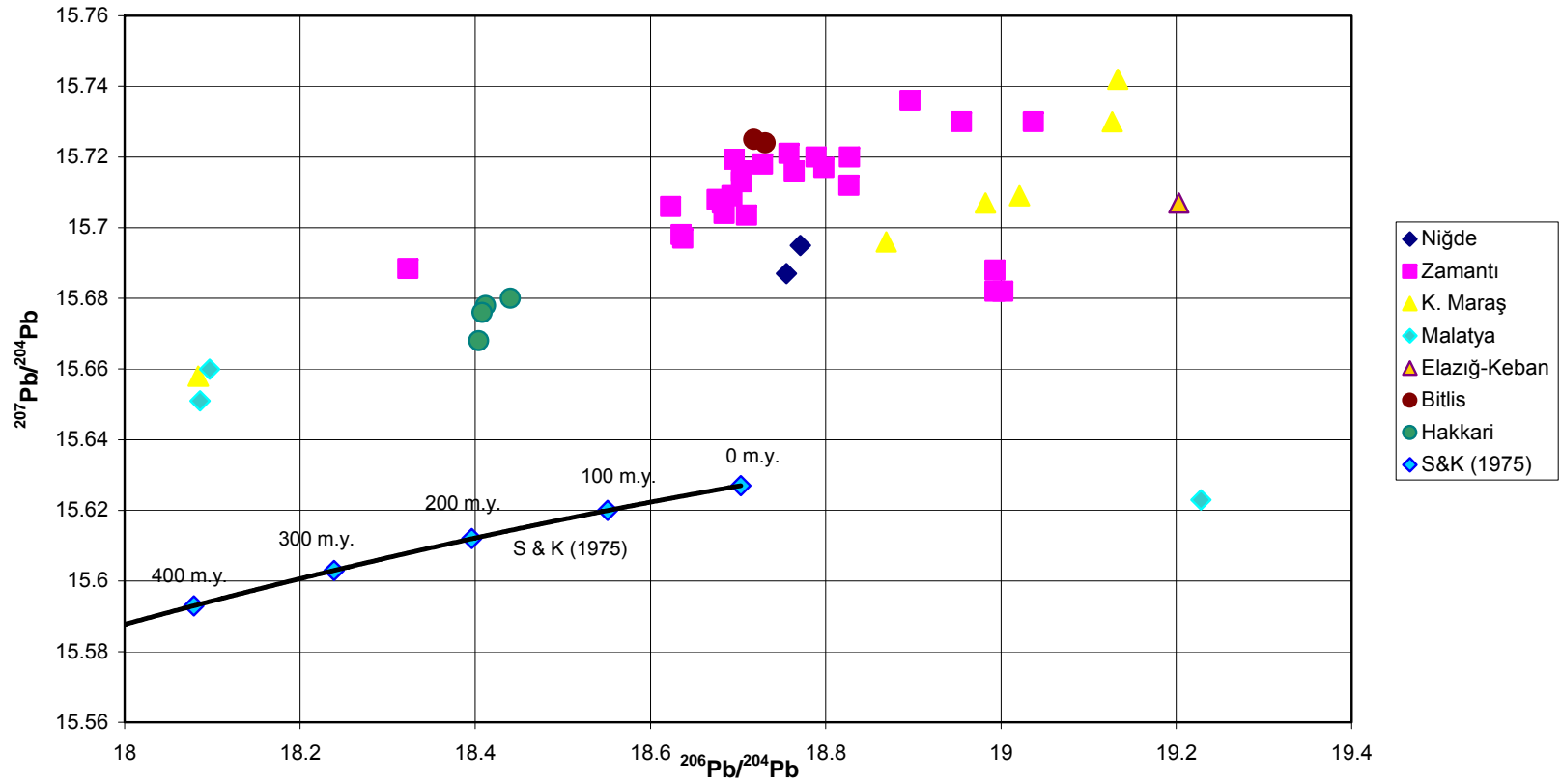


Figure 5.1. Positions of Pb-isotope data on uranium diagram. S&K (1975) : Average crustal growth curve of Stacey & Kramers (1975).

### Thorogenic Diagram

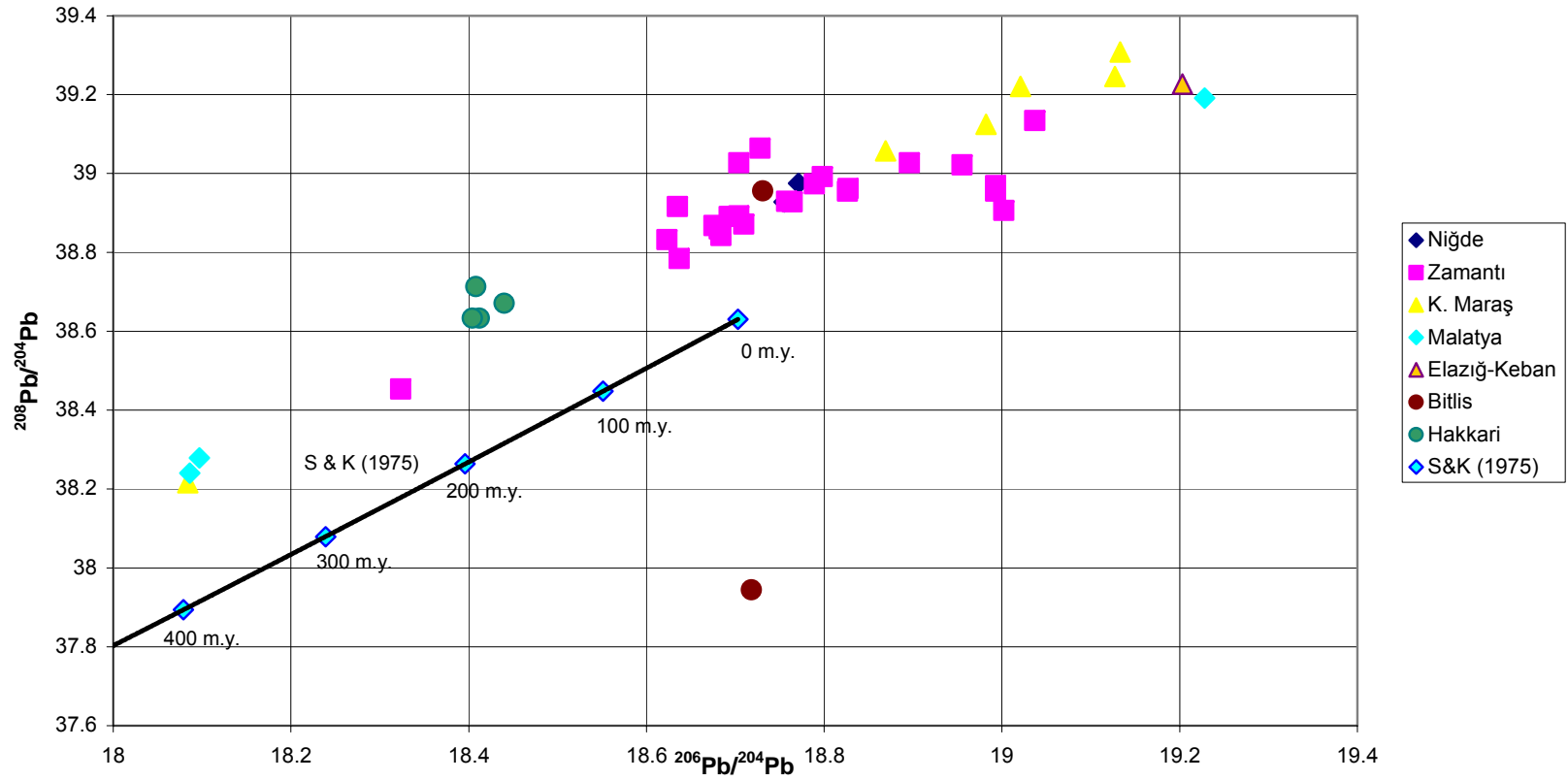


Figure 5.2. Positions of Pb-isotope data on thorogenic diagram. S&K (1975) : Average crustal growth curve of Stacey & Kramers (1975).

## CHAPTER 6

### DISCUSSION

#### 6.1. Introduction

The lead isotopic data on Table 5.1 was plotted on conventional Pb co-variation diagrams (Fig 6.1 and 6.2), together with reference crustal growth curves. Three growth curves are used for reference: average crustal growth curve of Stacey and Cramers (1975), Western Mediterranean growth curve (Arribas and Tosdal, 1994) and Turkey growth curve (Tosdal, 2001).

The crustal growth curves represent time integrated Pb-isotope composition of continental crust and are based on the use of U/Pb and Th/U ratios characteristic of a specific province, or of an average crust. The average crustal growth curve of Stacey and Cramers (1975) is based on a two stage-evolution of continental crust, each stage being characterized by different U/Pb and Th/U ratios. In the first stage the evolution of Pb starts 4.57 Ga ago with primordial isotope ratios which are recorded in troilite of the iron meteorite in Canyon Diablo (Tatsumoto et al., 1973). The second stage starts with geochemical differentiation of the first reservoir 3.70 Ga ago (differentiation of the crust from primordial mantle) with a change in the U/Pb and Th/U ratios of the reservoir (Table 6.1). The establishment of the growth curve based on these U/Pb and Th/U ratios uses the following equations:

$$(^{206}\text{Pb}/^{204}\text{Pb})_{t_1} = (^{206}\text{Pb}/^{204}\text{Pb})_{t_0} + (^{238}\text{U}/^{204}\text{Pb}) (e^{\lambda^{238}t_0} - e^{\lambda^{238}t_1})$$

$$(^{207}\text{Pb}/^{204}\text{Pb})_{t_1} = (^{207}\text{Pb}/^{204}\text{Pb})_{t_0} + (^{235}\text{U}/^{204}\text{Pb}) (e^{\lambda^{235}t_0} - e^{\lambda^{235}t_1})$$

$$(^{208}\text{Pb}/^{204}\text{Pb})_{t_1} = (^{208}\text{Pb}/^{204}\text{Pb})_{t_0} + (^{232}\text{Th}/^{204}\text{Pb}) (e^{\lambda^{232}t_0} - e^{\lambda^{232}t_1})$$

where

$\lambda$ ,  $\lambda'$ , and  $\lambda''$  are the decay constants of  $^{238}\text{U}$ ,  $^{235}\text{U}$ , and  $^{232}\text{Th}$ , respectively

$t_0$  and  $t_1$  correspond to the starting and ending times of growth stages, respectively

$(^{206}\text{Pb}/^{204}\text{Pb})_{t_1}$ ,  $(^{207}\text{Pb}/^{204}\text{Pb})_{t_1}$ ,  $(^{208}\text{Pb}/^{204}\text{Pb})_{t_1}$  are the ratios at time  $t_1$

$(^{206}\text{Pb}/^{204}\text{Pb})_{t_0}$ ,  $(^{207}\text{Pb}/^{204}\text{Pb})_{t_0}$ ,  $(^{208}\text{Pb}/^{204}\text{Pb})_{t_0}$  are the initial ratios (Table 6.1)

Table 6.1. Two-stage parameters for average active terrestrial lead (Stacey and Kramers, 1975)

	Time (b.y.)	$^{206}\text{Pb}/^{204}\text{Pb}$	$^{207}\text{Pb}/^{204}\text{Pb}$	$^{208}\text{Pb}/^{204}\text{Pb}$	U/Pb	Th/Pb	Th/U
start 1st stage	4.57	9.307	10.294	29.487	7.19	33.21	4.62
start 2nd stage	3.70	11.152	12.998	31.230	9.74	36.84	3.78
present day	0.00	18.700	15.628	38.630	9.74	36.84	3.78

The Western Mediterranean growth curve was established by Arribas and Tosdal (1994) using Pb isotopic data obtained from sulphide minerals in sedimentary rock-hosted ore deposits between Spain and Yugoslavia. This growth curve is based upon that established by Ludwig (1989) (Table 6.2) for sedimentary rock-hosted deposits in Sardinia. Turkey growth curve (Tosdal, 2001) was calculated based upon the first stage of Western Mediterranean growth curve, followed by a second stage of growth using slightly different U/Pb (9.95) and Th/U (3.95) ratios (Table 6.3).

Table 6.2. Two-stage parameters used by Ludwig (1989)

	Time (b.y.)	$^{206}\text{Pb}/^{204}\text{Pb}$	$^{207}\text{Pb}/^{204}\text{Pb}$	$^{208}\text{Pb}/^{204}\text{Pb}$	U/Pb	Th/Pb	Th/U
start 1st stage	4,57	9,307	10,294	29,476	7,50	30,60	4,08
start 2 <sup>nd</sup> stage	3,570	11,496	13,364	31,323	9,80	39,98	4,08
present day	0,00	18,746	15,685	39,052	9,80	39,98	4,08

Table 6.3. Two-stage parameters used by Tosdal (2001)

	Time (b.y.)	$^{206}\text{Pb}/^{204}\text{Pb}$	$^{207}\text{Pb}/^{204}\text{Pb}$	$^{208}\text{Pb}/^{204}\text{Pb}$	U/Pb	Th/Pb	Th/U
start 1st stage	4,57	9,307	10,294	29,476	7,50	30,60	4,08
start 2 <sup>nd</sup> stage	3,570	11,496	13,364	31,328	9,95	39,303	3,95
present day	0,00	18,857	15,721	38,920	9,95	39,303	3,95

The configuration of any data point on Pb co-variation diagrams, with regard to the reference crustal curves, can be used to discuss the age and source of mineralization. As discussed in Chapter 2, the compositional variations in  $^{206}\text{Pb}/^{204}\text{Pb}$  ratios are a function of time or age of formation, whereas the relative input of primitive versus old crustal Pb are recorded by the  $^{207}\text{Pb}/^{204}\text{Pb}$  values .

## 6.2. Pb-Isotope Compositional Groups: Implications as to the Age and Source of Mineralization

The lead isotopic composition of all the studied deposits plot above the average crustal growth curve of Stacey and Kramers (1975). Although Western Mediterranean and Turkey growth curves encompass most of the data points, some of the compositions plot at higher  $^{206}\text{Pb}/^{204}\text{Pb}$  beyond the 0-age (present day) making the use of Pb isotopic compositions for an absolute chronology almost impossible.

With regard to the compositional variations and the spatial distribution of the Pb-isotopic ratios, an inspection of Fig. 6.1. and 6.2. reveals, at a first sight, the presence of roughly five groups defined by the samples belonging to

1. Cafana (Malatya) and Türksevin (K. Maraş),
2. Kaleköy (Zamantı),
3. Hakkari,
4. Bitlis-Zizan, Niğde and most of the occurrences in Zamantı
5. K.Maraş-Afşin, Elazığ-Keban, some of the occurrences (Oreks, Ağcaşar, Dünderli and skarn-type) of Zamantı areas,

### Uranogenic Diagram

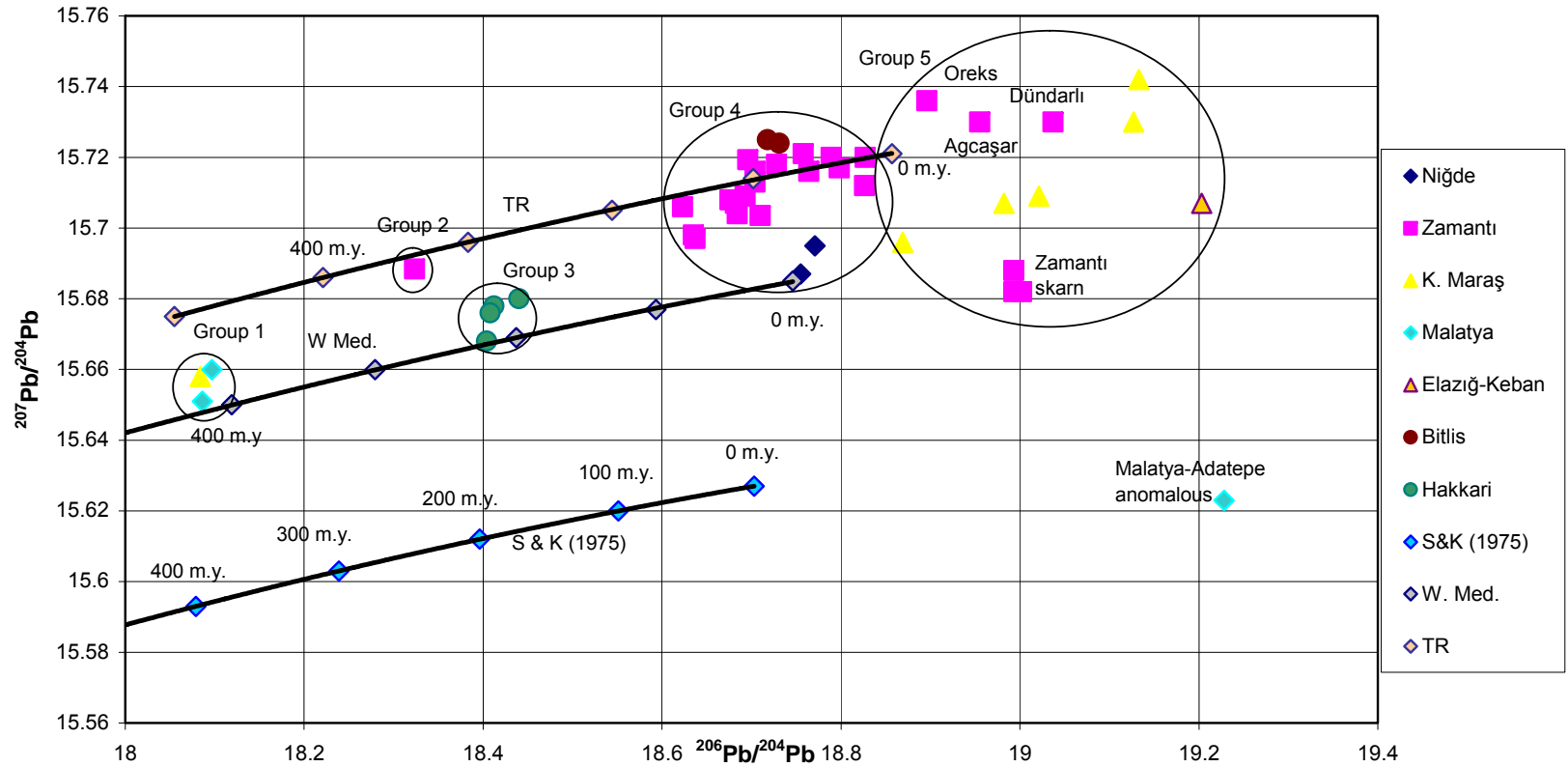


Figure 6.1. Pb-isotope groups on uranogenic diagram. S&K (1975) : Average crustal growth curve of Stacey & Kramers (1975). W. Med: Western Mediterranean growth curve from Arribas & Tosdal (1994), TR: Turkey growth curve from Tosdal (2001).

### Thorogenic Diagram

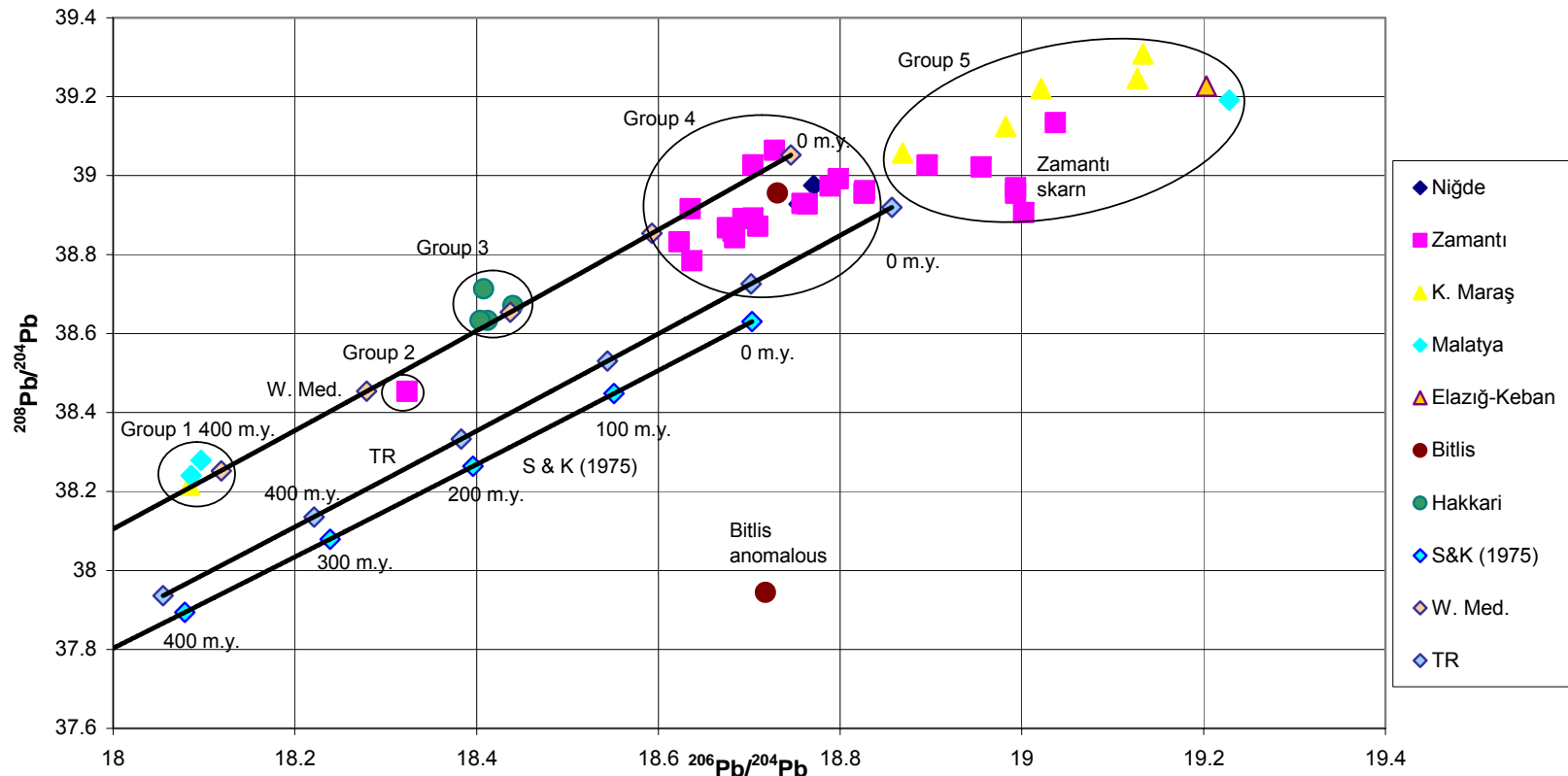


Figure 6.2. Pb-isotope groups on thorogenic diagram. S&K (1975) : Average crustal growth curve of Stacey & Kramers (1975). W. Med: Western Mediterranean growth curve from Arribas & Tosdal (1994), TR: Turkey growth curve from Tosdal (2001)

Adatepe and one of the Zizan samples have anomalous compositions out of these five groups.

The grouping given above is particularly relevant to the  $^{206}\text{Pb}/^{204}\text{Pb}$  variations which essentially reflects the variations in age owing to the long half life of  $^{238}\text{U}$  as compared to  $^{235}\text{U}$ . In this respect the transition from group number 1 to 5, suggest a decrease in the age of mineralization. Furthermore, high  $^{207}\text{Pb}/^{204}\text{Pb}$  ratios of all occurrences that lie above the average crustal growth curve of S&K (1975) indicate upper crustal Pb source.

### **6.2.1. Group 1**

The first group consists of Cafana (Malatya) and Türksevin (K.Maraş) deposits and is characterized by the lowest  $^{206}\text{Pb}/^{204}\text{Pb}$ ,  $^{207}\text{Pb}/^{204}\text{Pb}$ ,  $^{208}\text{Pb}/^{204}\text{Pb}$  ratios as compared to the other groups. Pb isotope compositions of these deposits lie along the Western Mediterranean growth curve and these deposits probably derived their Pb from a rock terrain characterized by U/Pb and Th/U ratios like those which defined the Western Mediterranean growth curve. According to the  $^{206}\text{Pb}/^{204}\text{Pb}$  ratios, which plot to the left of 400 Ma on the Western Mediterranean growth curve, the deposits are likely Paleozoic in age.

The inferred Paleozoic age for the Türksevin deposit, taken together with the fact that the deposit is hosted by Periman metamorphics (see Chapter 3 and Table 5.1), suggests syngenetic (SEDEX type) mineralization. However, it is not possible to reach a definite conclusion as vein type mineralizations were observed in the field by Teck Cominco geologists and Önal (1992) suggested ore formation by hydrothermal processes related to Paleocene volcanism.

### **6.2.2. Group 2**

The second group contains only Kaleköy deposit of Zamantı. The Pb isotope composition of the deposit lies close to the Turkey growth curve, on which most of the Zamantı deposits are located (particularly on  $^{206}\text{Pb}/^{204}\text{Pb}$  vs.  $^{207}\text{Pb}/^{204}\text{Pb}$  plot in Fig. 6.2), indicating the same source of Pb. However it has lower  $^{206}\text{Pb}/^{204}\text{Pb}$ ,

$^{207}\text{Pb}/^{204}\text{Pb}$  and  $^{208}\text{Pb}/^{204}\text{Pb}$  ratios than Pb isotope ratios of the other Zamantı deposits. The position with respect to the reference isochrons suggests that the Kaleköy deposit is likely Late Paleozoic-Early Mesozoic in age. This, together with the fact that mineralization is hosted by Paleozoic carbonates (Table 5.1), suggests syngenetic-early epigenetic mineralization for the Kaleköy deposit and does not contradict the statement by Vache (1964, 1966) that the deposit is SEDEX (Sedimentary Exhalative) type.

### **6.2.3. Group 3**

Hakkari deposits lie along the Western Mediterranean growth curve and these deposits probably derived their Pb from a rock terrain characterized by U/Pb and Th/U ratios like those of group 1. However Hakkari deposits have higher  $^{206}\text{Pb}/^{204}\text{Pb}$  ratios in comparison to group 1, and plot around 200 Ma on the Western Mediterranean growth curve, suggesting younger (Mesozoic) age for the mineralization.

Since the the occurrences in the area are conformable (stratabound) with Mesozoic limestones (see Chapter 3 and Table 5.1), the Mesozoic age obtained from the Pb-isotope data suggests syngenetic type mineralization.

### **6.2.4. Group 4**

The fourth group consists of Bitlis-Zizan, Niğde and most of the occurrences in Zamantı. The Pb-isotope ratios of the Zamantı and Zizan areas lie along the Turkey growth curve, whereas Niğde occurrences lie along the Western Mediterranean growth curve. The group has higher  $^{206}\text{Pb}/^{204}\text{Pb}$  that is close to the 0-age suggesting young (Cenozoic) Pb-model ages.

All the occurrences in this group have pre-Cenozoic host rocks (Chapter 3 and Table 5.1) and the Cenozoic age obtained from Pb-isotope data suggests epigenetic type mineralization.

### 6.2.5. Group 5

The most important characteristic of the group is that all the Pb-isotope ratios of this group plot beyond 0-age points of reference curves.

Since the host rocks of this group are all Pre-Cenozoic in age (except Çiğdem and Çal occurrences of K. Maraş) (Chapter 3 and Table 5.1), the configuration of the data on Pb co-variation diagrams (beyond 0-age) suggests epigenetic type mineralization.

Tosdal (2001), in his report on the Pb-isotope composition of sulphides from Turkey, suggested that the higher  $^{206}\text{Pb}/^{204}\text{Pb}$  ratios of these deposits indicate that their sources have higher U/Pb than other deposits in the Western Mediterranean, the higher  $^{206}\text{Pb}/^{204}\text{Pb}$  terrane reflecting largely magmatic Pb whereas lower  $^{206}\text{Pb}/^{204}\text{Pb}$  reflecting basement derived Pb as noticed in Spain. According to Tosdal (2001),  $^{207}\text{Pb}/^{204}\text{Pb}$  ratios of such magmatic related deposits may also be a measure for “magmatic-derived” vs. “basement-derived” Pb: Lower  $^{207}\text{Pb}/^{204}\text{Pb}$  may indicate a higher magmatic component, whereas higher  $^{207}\text{Pb}/^{204}\text{Pb}$  may indicate a greater involvement with the crustal column, either within the magmatic or hydrothermal system.

The argument by Tostal (2001), that these deposits have a magmatic input, is in fact supported by the observation that most of these deposits are associated with igneous rocks: the occurrences (to the south of Çadırkaya Fe-deposit) in Zamantı are skarn-type mineralizations spatially associated with andesites (Table 5.1); K. Maraş deposits (except Türksevin, involved in Group No.1, and Engizek) are hosted by andesitic, granitic and ophiolitic rocks (Table 5.1); Keban mineralization is associated with syenitic intrusions (Chapter 3). Although Yılmaz (1992) suggested SEDEX/MVT deposit for Keban mineralization, the mineralization was later affected by the syenitic intrusion during remobilization. Within the framework of the argument about the  $^{207}\text{Pb}/^{204}\text{Pb}$  ratios of these high  $^{206}\text{Pb}/^{204}\text{Pb}$  deposits, it can be suggested that the involvement of magmatic component (relative to crustal/basement-derived Pb) appears to be the highest in the skarn-type occurrences of Zamantı area.

### **6.2.6. Anomalous Compositional Group**

Malatya-Adatepe and one of the Bitlis-Zizan deposits constitute this group. The former one has an anomalously low  $^{207}\text{Pb}/^{204}\text{Pb}$  and the latter one has an anomalously low  $^{208}\text{Pb}/^{204}\text{Pb}$  ratio. The isotopic compositions of these deposits look rather suspicious and may have inherited some analytical errors. Therefore, the compositions of these deposits should be reanalysed before making any interpretation.

### **6.3. Comparison with Pb-Isotope Data from Selected Countries**

A further evaluation of the Pb-isotope composition of the studied deposits is made here in terms of correlation with the compositions of Pb-Zn occurrences from different provinces. The Pb-isotope data from four different occurrences in the Mediterranean Belt (from France, Spain, Saudi Arabia and Iran) are selected for this correlation. The data relevant to these occurrences plotted in Fig. 6.3 together with the data obtained in this study.

Stacey et al. (1980) report Pb isotopic analyses on a number of galena and whole-ore samples from base metal deposits in the Arabian Shield and concluded that they were largely deposited in an intraoceanic-arc environment. The Pb-isotope results lie in the emergence of a 700-750 m.y.- model Pb age bracket for the deposits (Fig. 6.3).

Marcoux and Moleo (1991) studied Pb-isotope geochemistry of base metal sulfide deposits hosted by French Massif Central in France. The Pb-isotope fields defined by Permian Sb-veins and Early Jurassic Pb-Ba veins were also plotted in Fig. 6.3. The ultimate source of mineralization is of lithologic type meaning the extraction by hydrothermal fluids of diffuse preconcentrations of metals at the scale of a geologic unit.

Gilg et al. (2003) reported that Angouran Zn oxide-sulfide deposit located in Iran hosted by a Neoproterozoic metamorphic complex of mostly marbles and schists. Sulfide ores are interpreted as a MVT type deposit probably related to Miocene

thrusting. Pb-isotope data from ores are homogeneous and indicate an upper crustal Pb source and young (Cenozoic) Pb-model ages.

The Pb-isotope data obtained from the studied deposits from France and Iran by Marcoux and Moleo (1991) and Gilg et al. (2003), respectively, lie above the crustal growth curve of Stacey and Kramers (1975) indicating an upper crustal Pb source for the deposits concerned. On the other hand, the Pb-isotope data from Arabian Shield, studied by Stacey et al. (1980), plot below the growth curve of Stacey and Kramers (1975) suggesting mantle-derived Pb source (Fig. 6.3).

The Pb-Isotope data from Spain is from Arribas and Tosdal (1994). The Pb-isotope data from the occurrences studied in this thesis plot close to those from France, Spain and Iran. The Pb-isotope field defined by Permian Sb-veins of France is located close to the Cafana and Tüksevin occurrences suggesting that the mineralization ages of the deposits are close to each other. The Pb-isotope field defined by Early Mesozoic deposits of Spain is very close to Kaleköy-Zamantı occurrence. The Pb-isotope field defined by Early Jurassic Pb-Ba veins of France is very close to Hakkari occurrences. The Miocene Angouran (Iran) deposit has Pb-Isotope data plotted close to the studied (skarn-type) Zamantı and Afşin-K. Maraş occurrences confirming Cenozoic age of mineralization for these areas. Overall, the data from Turkey have a configuration on the Pb co-variation diagram similar to those from France, Spain and Iran (above the crustal growth curve of Stacey and Kramers (1975)), indicating derivation of Pb largely from an upper crust.

#### **6.4. Final Comments**

The Pb-isotope compositions reveal that for most of the Pb-Zn occurrences in the Tauride-Anatolide Belt, as well as in the Hakkari area, the source of mineralization is essentially crustal regardless of the age, although magmatic input appears to have contribution to some of the deposits which are spatially associated with igneous rocks. This distinction as to the source of mineralization (basement vs magmatic source) seems-within the limits of available Pb-isotope data-to be independent of geographic and/or tectonic control. While some of the

### Uranogenic Diagram

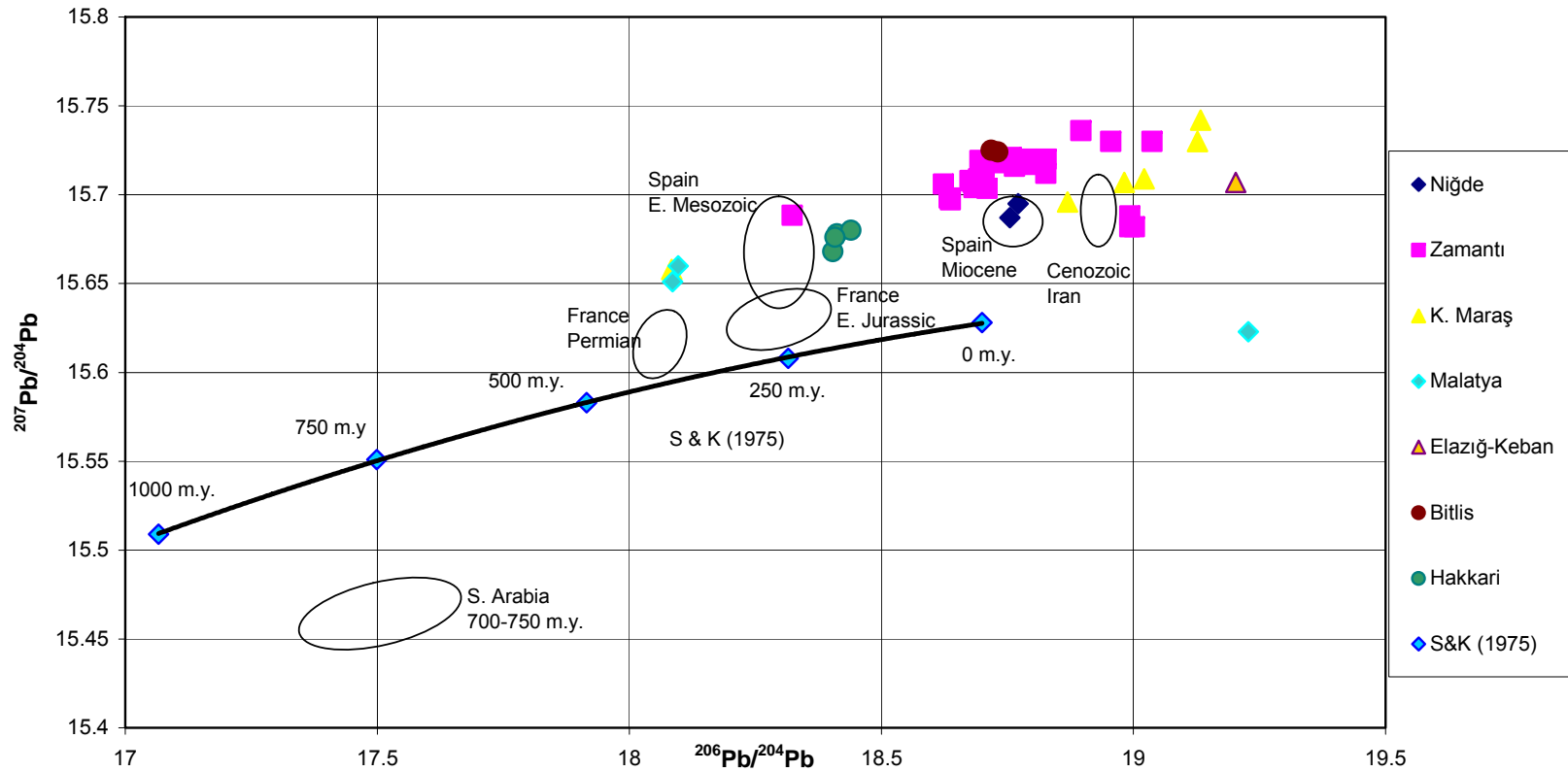


Figure 6.3. Pb-isotope data on uranogenic diagram with the Pb-isotope fields of S. Arabia, Fance, Spain and Iran are from Bokhari and Kramers (1982), Marcoux and Moelo (1991), Arribas and Tosdal (1994) and Gilg et al. (2003) respectively. S&K (1975) : Average crustal growth curve of Stacey & Kramers (1975).

occurrences in Zamantı (e.g., Kaleköy) and K. Maraş (e.g., Türksevin) have an essentially crustal source, other occurrences in the same areas (e.g. Oreks, Dünderlı, Ağcaşar-Zamantı and Afşin-K. Maraş) appear to have magmatic input. Likewise, not only the occurrences in Taurides (e.g., Zamantı, K. Maraş, Malatya) but also those in the Arabian Platform (Hakkari) seem to be dominated by crustal contribution.

As to the age of mineralization, 5 major groups of occurrences emerges from the Pb-isotope compositions: Paleozoic (Cafana-Malatya and Türksevin-K.Maraş), Late Paleozoic-Early Mesozoic (Kaleköy-Zamantı), Mesozoic (Hakkari), Cenozoic (most of the occurrences in Zamantı and Niğde) and those plotting beyond the 0-age isochron (Afşin-K. Maraş; Oreks, Dünderlı, Ağcaşar, skarn type deposits to the south of Çadirkaya-Zamantı; Keban-Elazığ). The latter is the group inferred to have magmatic contribution in their genesis. Like it is the case with the source of mineralization, there does not seem to be geographic and/or tectonic control in this distinction.

When taken together with the reported ages of host rocks, the ages and the source of mineralizations inferred from the Pb-isotope data can also be used to make a distinction between syngenetic and epigenetic type mineralizations as long as it is supported by field observations. In this respect, the inferred syngenetic origin for Hakkari area seems to hold as the occurrence is observed as stratabound deposits. Likewise most of the epigenetic occurrences inferred from Pb-isotope data are indeed the ones observed as veins & karstic / fracture fillings in the field (e.g., most of the Zamantı and Niğde deposits)

The Pb-Zn occurrences in Turkey have Pb-isotope compositions similar to those from other occurrences in the Mediterranean Belt (e.g. Spain, France, Iran), reflecting –to a large extent– the characteristics of the crustal basement—a term, that is used here to refer to the basement, as well as the crustal column traversed by hydrothermal solutions.

## CHAPTER 7

### CONCLUSIONS AND RECOMMENDATIONS

- Pb-isotope composition of galena minerals from the studied Pb-Zn occurrences delineates 5 major groups defined by the samples belonging to:
  1. Cafana (Malatya) and Türksevin (K. Maraş),
  2. Zamantı-Kaleköy,
  3. Hakkari,
  4. Bitlis-Zizan, Niğde and most of the occurrences in Zamantı,
  5. K.Maraş-Afşin, Elazığ-Keban, and some of the occurrences (Oreks, Ağcaşar, Dünderli and skarn type deposits to the south of Çadırkaya) in Zamantı areas.
- The configuration of the data points with regard to the reference isochrons on Pb-isotope diagrams yield Paleozoic, Late Paleozoic-Early Mesozoic, Mesozoic and Cenozoic ages for Group no. 1, 2, 3 and 4-5, respectively.
- All the occurrences have Pb-isotopic ratios suggesting upper crustal Pb source.
- The occurrences comprising Group no.5 and plotting beyond the 0-age isochron on isotope co-variation diagrams, appear to have magmatic contribution in their genesis.
- This distinctions as to the age and source (basement vs. magmatic) of mineralizations seems to be independent of geographic and/or tectonic control. However, this is a tentative conclusion reached within the limits imposed by relatively restricted number of samples available for some localities.
- When taken collectively with the reported ages of host rocks, the ages and sources of mineralization obtained from the Pb-isotope data suggest Cenozoic aged epigenetic mineralization for most of the Zamantı, Niğde and Keban deposits, and Mesozoic syngenetic mineralization for Hakkari

area. For the rest of the deposits, the inferred type of mineralization should be checked by further chronological studies (particularly on wall rocks and alteration products), and the studies on mineralization characteristics, geochemistry, alteration and fluid chemistry.

- The Pb-Zn occurrences in Turkey have Pb-isotope compositions similar to those from other occurrences in the Mediterranean Belt (e.g. Spain, France, Iran).
- The isotopic compositions of Bitlis-Zizan and Malatya-Adatepe deposits look rather suspicious and may have inherited some analytical errors. Therefore, the compositions of these deposits should be reanalysed before making any interpretation.
- For a better understanding of the genesis of ore deposits, it is highly recommended that the future studies should be directed to the Pb-isotope composition of the wall rocks and the basement. This will lead to the development of a quantitative modelling of i) the relative contribution of the possible sources to ore genesis, as well as ii) the interaction between hydrothermal fluids and the wall rock.

## REFERENCES

- Adıgüzel, O., Sarı, İ., ve Baysal, M., 1991, K.Maraş-Elbistan-Çardak-Ericek-Berit Dağı yöresi demir yatakları maden jeolojisi raporu, MTA, Ankara.
- Akiman, O., Erler, A., Göncüoğlu, M. C., Güleç, N., Geven, A., Türeli, K., and Kadioğlu, Y. K., 1993, Geochemical characteristics of granitoids along the western margin of the Central Anatolian Crystalline Complex and their tectonic implications: *Geological Journal*, v. 28, p. 371-382.
- Allegre, C. J., Hart, S. R., and Dupre, B., 1988, A coherent crust-mantle model for the uranium-thorium-lead isotopic system: *Chemical Geology*, v. 70, p. 211-234.
- Altiner, D., 1989, An example for the tectonic evolution of the Arabian Platform margin (SE Anatolia) during the Mesozoic and some criticisms of the previously suggested models, in Şengör, A. M. C., ed., *Tectonic evolution of the Tethyan regions*: Dordrecht, Netherlands, Kuwer academic Publishing, p. 117-129.
- Altınlı, İ. E., 1953, Hakkari güneyinin jeoloji incelemesi, TPAO Rap. No: 98
- Arribas, Jr. A., and Tosdal, R. M., 1994, Isotopic composition of Pb and S in base - and precious-metal deposits of the Betic Cordillera, Spain: Origin and relationship to other European deposits: *Economic Geology*, v. 89, p. 1074-1093.
- Ayhan, A., 1983, Genetic comparison of lead-zinc deposits of Central Taurus: 1. *International Symposium of Taurus belt*, Ankara, p. 335-342.
- Balçık, A., 1979, Keban Nallıziyaret ve Karamağara Dere (Bamas) cevherleşmesi, MTA Rap. 6675, (yayımlanmamış), Ankara.

- Bjorlykke, A. and Sangster, D. F., 1981. An overview of sandstone leaddeposits and their relation to red-bed copper and carbonate hosted lead - zinc deposits. *Economic Geology*, Seventy Fifth Anniversary Volume, 179-213.
- Blumenthal, M. M., 1952, Das taurische Hochgebirge des Aladağ, neuere Forschungen zu seiner Geographie, Stratigraphie und Tektonik: Maden Tetkik ve Arama Enst. Ankara: seri D, 136 s.
- Bokhari, F. Y. and Kramers, J., 1982. Lead isotope data from massive sulfide deposits in the Saudi Arabian Shield. *Economic Geology*, 75, 1766-1769
- Bozkurt, E., and Mittwede, S. K., 2001, Introduction to the Geology of Turkey-A synthesis, *International Geology Review*, v. 43, p. 578-594.
- Çağlayan., H., 1984, Die Vererzung der Fluorit-Molybdanglanzführenden Blei-Zink-Lagerstätten von Keban-Elazığ im Südost-Taurus (Türkei): Ph. D. Theises Univ. Vienna.
- Cannon, R. S., Jr., Pierce, A. P., Antweiler, J. C., and Buck, K. L., 1961, The data of lead isotope geology related to problems of ore genesis: *Economic Geology*, v. 56, p. 1-38.
- Cengiz, R., Yılmaz, H., ve Türkyılmaz, B., 1991, Çinkur'a ait ÖİR-671 ve ÖİR-1714 no'lu Malatya-Yeşilyurt-Görgü (Cafana) ruhsat sahaları jeoloji etüdü sonuç raporu, MTA, Ankara (in Turkish).
- Çevrim, M., Echle, W., and Friedrich, G., 1986, Paleokarst related Zn-Pb mineralization of Aladağ Mountains, *Bulletin of the Geological Society of Turkey*, v. 29, p. 27-41.

- Cumming, G. L., and Richards, J. R., 1975, Ore lead in a continuously changing earth: *Earth and Planetary Science Letters*, v. 28, p. 155-171.
- Davidson, J. P., 1996, Deciphering mantle and crustal signatures in subduction zone magmatism: *American Geophysical Union Monograph* 96, p. 251-262.
- Dickin, A.P., 1995. *Radiogenic Isotope Geology*, Cambridge, Cambridge University Press, 490 p.
- Doe, B. R., 1970. *Lead Isotopes*: New York, Springer-Verlag, 137 p.
- Doe, B. R., and Zartman, R.E., 1979. *Plumbotectonics 1: The Phanerozoic* in: Barnes, H. L., (ed), *Geochemistry of Hydrothermal Ore Deposits*, Wiley, New York, 22-70
- Faure, G., 1977, *Principles of Isotope Geology*: New York, John Wiley & Sons, 464 p.
- Frech, F., 1916, *Geologie Kleinasiens im Bereich der Bağdadbahn*: *Zeitschrift d. D tsch. Geol. Ges. Abhandlungen*.
- Garipey, C., and Dupre, B., 1991, Pb-isotopes and crust-mantle evolution: *Mineralogical Association of Canada Short Course handbook*, v. 19, p. 191-224.
- Gautier, P., Bozkurt, E., Hallot, E., Dirik, K., 2002, Dating the exhumation of a metamorphic dome: geological evidence for pre-Eocene unroofing of the Nigde Massif (Central Anatolia, Turkey): *Geological Magazine*, v. 139 (5), p. 559-576.
- Gawlik, J., 1958, *Keban (Elazığ) prospeksiyon raporu*: MTA Rap. 384, (yayımlanmamış), Ankara

- Geoffroy, J. de., 1960, Keban kurşun ve çinko madeni satıhta ve yer altında maden arama programı, MTA.
- Gilg, H. A., Allen, C., Balassone, G., Boni, M., and Moore, F., 2003, The 3-stage evolution of Angouran Zn 'oxide'-sulfide deposit, Iran: Mineral Exploration and Sustainable Development, Eliopoulos et al. eds., p. 77-80.
- Göncüoğlu, M. C., 1982, Zircon U/Pb ages from pargneisses of the Niğde massif (Central Anatolia), Geol. Soc., Turkey Bull., 25, 61-66.
- Göncüoğlu, M. C., 1984, The metamorphism and age of the Muş-Kizilagic metagranite: MTA Bull, 99/100, 37-48.
- Göncüoğlu, M. C., 1986, Orta Anadolu Masifi'nin güney ucundan jeokronolojik yas bulguları: Mineral Resource and Exploration Institute of Turkey (MTA) Bulletin, v. 105/106, p. 111-124 (in Turkish with English abstract).
- Göncüoğlu, M. C., Toprak, V., Kuşçu, I., Erler, A., and Olgun, E., 1991, Orta Anadolu Masifi'nin batı bölümünün jeolojisi, Bölüm 1: Güney Kesim: Turkish Petroleum Corporation Report no 2909, 140 p (in Turkish).
- Göncüoğlu, M. C., Erler, A., Toprak, V., Yalınz, K., Olgun, E., and Rojay, B., 1992, Orta Anadolu Masifinin Batı Kesiminin Jeolojisi, Bölüm II. Orta Kesim: TPAO Rap. No: 3155, 76 p.
- Göncüoğlu, M. C., and Türeli, T. K., 1984, Alpine collisional-type granitoids from Central Anatolian Crystalline Complex, J. of Kocaeli Uni., 1, 39-64.
- Göncüoğlu, M. C., Dirik, K., and Kozlu, H., 1996-1997, Pre-Alpine and Alpine Terranes in Turkey: Explanatory notes to the terrane map of Turkey, *Annates Geologiques des Pays helleniques*, 37, 515-536, Athenes.

- Göncüoğlu, M. C., and Turhan, N., 1997, Rock units and metamorphism of the basement and Lower Paleozoic cover of the Bitlis Metamorphic Complex, SE Turkey: Turkish Association of Petroleum Geologists Special Publication No:3, Ankara.
- Göncüoğlu, M. C., Turhan, N., Sentürk, K., Özcan, A., Uysal, S., and Yaliniz, M. K., 2000, A geotraverse across northwestern Turkey: Tectonic Units of the Central Sakarya region and their tectonic evolution, in Bozkurt, E., Winchester J. A., and Piper, J. D. A., eds., Tectonic and magmatism in Turkey and the surrounding area: Geological Society of London, Special Publication, no. 173, p. 139-161.
- Granning, ., 1934, (Keban) nam mahalddeki altın ve gümüş madeni hakkında rapor, MTA, derleme no: 6759 k., Ankara.
- Gulson, B.L., 1986, Lead isotopes in mineral exploration: Amsterdam, Elsevier, 245 p.
- Güleç, N., 1994, Rb-Sr isotope data from the Agaçören granitoid (east of Tuzgölü): Geochronological and genetic implications: Turkish Journal of Earth Sciences, v. 3, p. 39-43.
- Hall, R., 1976, Ophiolite emplacement and the evolution of the Taurus suture zone, southeastern Turkey, Geol. Soc. Of American Bull., v. 87, p. 1078-1088.
- Henley, R. W., Truesdell, A. H., Barton, P. B., Jr., and Whitney, J. A. 1984, Fluid-mineral equilibria in hydrothermal systems: Society of Economic Geologists, Reviews in Economic Geology, v. 1, 267 p.

- Helvacı, C., and Griffin, W. L., 1984, Rb/Sr geochronology of the Bitlis Massif, Avnik area, Geol. Soc. London Spec. Publ., 17, 403-413.
- Imrech, L., 1964, çamardı kuzeyindeki eski antimuan işletmeleri hakkında not: MTA derleme raporu no: 3749.
- Imrech, L., 1965, Zamantı metal cevherleşmesi bölgesinin kurşun-çinko mineralizasyonları, MTA Ens. Dergisi, Ankara, s. 65, ss. 85-109.
- Kadıoğlu, Y. K., Dilek, Y., Güleç, N., Foland, K. A., 2003, Tectonomagmatic evolution of bimodal plutons in Central Anatolian Crystalline Complex, Turkey: Journal of Geology, v. 111, p. 671-690.
- Kesler, S. E., Cumming, G. L., Krstic, D., and Appold, M. S., 1994, Lead isotope geochemistry of Mississippi Valley-type deposits of the southern Appalachians: Economic Geology, v. 89, p. 307-321.
- Ketin, I., 1966, Tectonic units of Anatolia (Asia Minor): Mineral Resource and Exploration Institute of Turkey (MTA) Bulletin, v. 66, p. 22-34
- Kovenko, V., 1944, Bor bölgesi inkişafı: MTA, derleme rapor no: 1391.
- Köksoy, M., 1972, Keban maddeni civarında cevherleşmeyle ilgili elementlerin dağılımı, MTA, derleme no:2402, Ankara.
- Köksoy, M., 1978, Relationship between geological, geophysical and geochemical data obtained from blind lead-zinc mineralization at Keban, Turkey, Journal of Geochemical Exploration, v. 9, p. 39-52.
- Lengeranlı, Y., 1982-1983, Yahyalı (Kayseri) doğusu ile Hoşça-Çataloluk (Kaayseri-Develi) köyleri güneyinin jeolojisi ve kurşun-çinko cevherleşmeleri etüd raporu, MTA, Ankara.

- Le Huray, A.P., 1982. Lead isotopic patterns of galena in the Piedmont and Blue Ridge ore deposits, southern Appalachians. *Economic Geology*, 77, 335-351.
- Ludwig, K. R., 1989, Isotopic constraints on the genesis of base-metal ores in southern and central Sardinia, *Eur. J. Mineral.*,1, 657-666.
- Ludwig, K. R., Vollmer, R., Turi, B., Simmons, K. R., and Perna, G., 1989, Isotopic constraints on the genesis of base-metal ores in southern Sardinia: *European Journal of Mineralogy*, v. 1, p. 657-666.
- Lugmair, G.W. and Marti, K., 1978. Lunar initial  $^{143}\text{Nd}/^{144}\text{Nd}$ : Differential evolution of the Lunar crust and mantle. *Earth and Planetary science letters*, 39, 349-357.
- Marcoux, E., and Moelo, Y., 1991, Lead isotope geochemistry and paragenetic study of inheritance phenomena in metallogenesis: examples from base metal sulfide deposits in France, *Economic Geology*, v. 86, p. 106-120.
- Metag, Stolberger Z., 1971, zamantı çinko-kurşun, projesi, nihai rapor: maden sahalarının jeolojisi, mineraloji-paleontoloji ekleri: DPT Müsteşarlığı, 177 sayfa (in Turkish).
- Metz, K., 1939, beitrage zue Geologie des Kilikischen Taurus im gebiete des Aladağ: *Sitz. Ber. Ak. Wien, Abt.*, 1, 148, 7-10.
- MTA, 1995, Kayseri ili ddoğal kaynaklar envanteri, Sivas
- Okay, A. I., 1986, High-pressure/low temperature metamorphic rocks of Turkey: *Geological Society of America Buletin*, v. 164, p. 333-347

- Okay, A. I., 1989, An exotic eclogitic/blueschist slice in a Barrovan-style metamorphic terrain, Alanya nappes, Southern Turkey: *Journal of Petrology*, v. 30, p. 107-132.
- Okay, A. I., and Özgül, N., 1984, HP/LT metamorphism and the structure of the Alanya Massif, southern Turkey, in Dixon J. E., and Robertson, A. H. F., eds, *The geological evolution of the Eastern Mediterranean: Geological Society of London, Special Publication, no. 17*, p. 429-439.
- Okay, A. I., and Tüysüz, O., 1999, Tethyan sutures of northern Turkey, in Durand, B., Jolivet, L., Horvath, D., and Serranne, M., eds., *The Mediterranean basins: Tertiary extension within the Alpine orogen: geological Society of London, Special Publication, no. 156*, p. 475-515.
- Önal, M., Tuzcu, N. and Helvacı, C., 1990, Geological setting, mineralogy and origin of the Cafana (Malatya) Zn-Pb sulfide and carbonate deposit, E Anatolia, Turkey, in: *Int. Earth Sci. Congress on Aegean Regions, Proceedings*, ed: M. Y. Savascın & A. H. Eronat, Izmir, D. E. University, v. 1, p. 52-58.
- Oygür, V., 1986, Karamadazı (Yahyalı-Kayseri) kontak metazomatik manyetit yatağının jeolojisi ve oluşumu: *jeoloji mühendisliği*, 27, p. 1-9.
- Özgül, N., 1976, Torosların bazı temel jeoloji özellikleri, *TJK Bülteni*, c. 19, p. 65-78 (in Turkish with English abstract).
- Özgül, N., 1981, Munzur dağlarının jeolojisi: MTA Rap. 6995, (yayımlanmamış), Ankara.

- Özgül, N., 1985, The geology of Alanya region, in Ketin Symposium: Ankara, Geological Society of Turkey Publication, p. 97-120 (in Turkish with English abstract).
- Özgüneyli, A., 1978, Niğdde-Çamardı Kristalin masifi genel prospeksiyon çalışması ve demir-baz metal-wolfram ve altın cevherleşmeleri hakkında çalışma raporu: MTA Maden etüd arşivi no: 1710.
- Öztunalı, Ö., 1985-1989, Etibank-Keban maden sahaları durum tespit raporları: Etibank Arşivi, 85 s., Ankara.
- Pehlivan, A. N., Alpan, T., Zaralıoğlu, M., Taş, N., ve Salta, N., 1986, Niğde Masifi altın kalay cevherleşmesi ve ağır mineral çalışmaları ön raporu, MTA, Balıkesir.
- Perinçek, D., 1980, Hakkari-Yüksekova-Çukurca-Beytüşşebab-Uludere Pervari dolayının jeolojisi, TPAO Rap. No: 1481, 80 s.
- Perinçek, D., 1990, Hakkari ili ve dolayının stratigrafisi, Güneydoğu Anadolu, Türkiye, TPJD Bulletin, v. 2/1, p. 21-68. (in Turkish with English abstract).
- Philippson, A., 1918, Kleinasien, Handdbuch der Regional Geologic: v. 2, Heidelberg.
- Richards, J. P., 1995, Alkalic-type epithermal gold deposits-a review: Mineralogical Association of Canada Short Course Handbook, v. 23, p. 367-400.
- Richards, J. P., McCulloch, M. T., Chappel, B. W., and Kerrich, R., 1991, Sources of metals in the Porgera gold deposit, Papua New Guinea: Evidence from alteration, isotope and noble gas geochemistry: Geochimica et Cosmochimica Acta, v. 55, p. 565-580.

- Sađırođlu, A., 1988, Cafana (Görgü), Malatya carbonated Zn-Pb deposits, Bulletin of the Faculty of Eng., Cum. Uni., serie A- Earthsciences, V. 5, N. 1. (in Turkish with English abstract).
- Sato, K., 1975. Unilateral isotopic variation of Miocene ore leads from Japon. Economic Geology, 70, 800-805
- Schaffer, F. X., 1903, Cilicia: Peterm. Mitt., Ergänzungsheft, 141.
- Şengör, A. M. C., and Yılmaz, Y., 1981, Tethyan evolution of Turkey: A plate tectonic approach: Tectonophysics, v 75, p. 181-241.
- Sengun, M., 1995, The metamorphism an the relationship between infra- and supra-structures of the Bitlis Massif, Turkey: Mineral Res. Exp. Bull, v. 115, p. 1-13.
- Seymen, I., 1981, Stratigraphy and metamorphism of the Kirsehir massif around Kaman (Kirsehir-Turkey): Geological Society of Turkey Bulletin, v. 24, p. 101-108 (in Turkish with English abstract).
- Stacey, J. S., and Kramers, J. D., 1975, Approximation of terrestrial leadisotope evolution by two-stage model: earth and Planetary Science Letters, v. 26, p. 207-221.
- Stacey, J. S., Doe, B. R., Roberts, R. J., Delevaux, M. H., and Gramlich, J. W., 1980, A lead isotope study of mineralisation in the Saudi Arabian Shield: Contr. Mineralogy Petrology, v. 74, p. 175-188.
- Steiger, R.H., and Jager, E., 1977. Subcomission on geochronology: convention on the use of decay constant in geo- and cosmochronology. Earth an Planetary Science Letters, 36, 359-362

- Stephan, A.K., and Geoffrey, F.P., 1982. Application of lead isotope studies to massive sulphide and vein deposits of the Caroline Slate Belt. *Economic Geology*, 77, 352-363
- Sündal, Ü., 1968, Keban flüorit cevherleşmesi, MTA, derleme no: 4056, Ankara.
- Tarhan, N., 1986, Evolution and Origin of granitoid magmas related to the closure of neo-Tethys in eastern Taurus (Turkey): *Bulletin, Mineral Research & Exploration Institute of Turkey*, v. 107, p. 38-60.
- Ttatumoto, M., Knight, R. J., and Allegre, C. J., 1973, Time differences in the formation of meteorites as etermined from the ratio of lead-207 to lead-206. *Science*, 180, p. 1279-1283.
- Tatumoto, M., 1978, Isotopic composition of lead in oceanic basalt and its implication to mantle evolution: *Earth and Planetary Science letters*, v. 38, p. 63-87.
- Taylor, S. R., and McLennan, S. M., 1985, *The continental crust: It's composition and evolution*: Oxford, Blackwell Scientific, 32p.
- Tekeli, O., 1980, Aladağlar'ın yapısal evrimi: *Türkiye Jeol. Kur. Bült.*, v. 23/1, p. 11-14.
- Tekeli, O., 1981, Aladağ ofiyolitli melanjinin özellikleri: *Türkiye Jeol. Kur. Bült.*, v. 24/1.
- Tekeli, O., Aksay, A., Evren-Ertan, İ., Işık, A., ve Ürgün, B. M., 1981, Toros ofiyolit projeleri Aladağ projesi raporu: MTA Gen. Md., Rapor No 6976 (yayınlanmamış).

- Tosdal, R., M., 2001, Sulfide Pb isotope from ore deposits and prospects in Turkey and Iran: Comments and observations prepared for Cominco Ltd, (not published).
- Tosdal, R. M., Wooden, J. L., and Bouse, R. M., 1999, Pb isotopes, ore deposits, and Metallogenic Terranes, Application of radiogenic isotopes to ore deposit research and exploration, *Reviews in Economic Geology*, v 12, p. 1-28.
- Tschihatschef, P., 1869, *Asie Mineure*, 1-3, Paris
- Türkunal, S., 1980, Doğu ve Güneydoğu Anadolu'nun Jeolojisi, *Jeoloji Müh. Odası Yayını*: 8, Ankara.
- Ulakoğlu, S., 1983, Karamadazı graniti ve çevresinin jeolojisi: *Jeol. Müh.*, 17, 69-78.
- Vache, R., 1964, antitoroslardaki Bakırdağ Kurşun Çinko Yatakları (Kayseri), *MTA dergisi*, s. 62, ss. 87-98 (in Turkish).
- Vache, R., 1966, Zur Geologie der Varisziden und ihre lagerstätten im südanatalischen Taurus: *Min. Dep.*, v. 1, p. 30-42.
- Whitney, D. L., Dilek, Y., 1997, Core complex development in central Anatolia, Turkey: *Geology*, v.25 (11), p. 1023-1026.
- Whitney D.L., Teyssier C., Dilek Y., Fayon AK., 2001, Metamorphism of the Central Anatolian Crystalline Complex, Turkey: influence of orogen-normal collision vs, wrench-dominated tectonics on P-T-t paths, *Journal of Metamorphic Geology*, 19, p. 411-432.

Wohryzka, K., 1966, Zur Geologie und metallogenese des Gebietes zwischen Yahyalı (Kayseri) and zamantı-fuB: MTA Derg, s. 67, ss. 97-104.

Yalçın, R., 1972, Keban fluorit sahasının etüdü, MTA.

Yaliniz, M. K., Aydın, N. S., Göncüođlu, M. C., and Parlak, O., 1999, Terlemez quartz monzonite of central Anatolia (Aksaray-Sarkaraman): Age, petrogenesis, and geotectonic implications for ophiolite emplacement: Geological Journal, v. 34, p. 233-242.

Yazgan, E., 1984, Geodynamic evolution of the eastern Taurus region, In: Tekeli, O. and Göncüođlu, M. C. (eds), Int. Symp. on the Geology of the Taurus Belt, Proceedings, Mineral. Res. Explor. Inst., Ankara, 199-208.

Yılmaz, A., Ünlü, T., Sayılı, S., 1992, Keban (Elazığ) kurşun-çinko cevherleşmelerinin kökenine bir yaklaşım: ön çalışma: MTA Dergisi, v. 114, p. 47-70.

Yılmaz, O., 1975, Petrographic and stratigraphic study of the rocks of the Cacas region (Bitlis massif): Türkiye Jeol. Kur. Bülteni., 18, 33-40.

Yılmaz, Y., 1993, New evidence and model on the evolution of the Southeast Anatolian orogen: Geological Society of the America Bulletin, v. 105, p. 251-271.

Zartman, R. E., and Doe, B. R., 1981, Plumbotectonics-the model: Tectonophysics,, v. 75, p. 135-162.

Ziserman, A., 1969, Geological and mining study of Keban Maden: Etibank Arşiv No: 123, 70s., Ankara.

APPENDIX A: Sample location and generalized geological map (modified from MTA 1:500000 geological maps, 1961).

